
Diagnostic Uncertainty Calibration: Towards Reliable Machine Predictions in Medical Domain

Takahiro Mimori
RIKEN AIP

Keiko Sasada
Kumamoto University Hospital

Hiroataka Matsui
Kumamoto University

Issei Sato
The University of Tokyo,
RIKEN AIP, ThinkCyte

Abstract

We propose an evaluation framework for class probability estimates (CPEs) in the presence of label uncertainty, which is commonly observed as diagnosis disagreement between experts in the medical domain. We also formalize evaluation metrics for higher-order statistics, including inter-rater disagreement, to assess predictions on label uncertainty. Moreover, we propose a novel post-hoc method called α -calibration, that equips neural network classifiers with calibrated distributions over CPEs. Using synthetic experiments and a large-scale medical imaging application, we show that our approach significantly enhances the reliability of uncertainty estimates: disagreement probabilities and posterior CPEs.

1 Introduction

The reliability of uncertainty quantification is essential for safety-critical systems such as medical diagnosis assistance. Despite the high accuracy of modern neural networks for a wide range of classification tasks, their predictive probability often tends to be uncalibrated (Guo et al., 2017). Measuring and improving probability calibration, i.e., the consistency of predictive probability for an actual class frequency, has become one of the central issues in machine learning research (Vaicenavicius et al., 2019; Widmann et al., 2019; Kumar et al., 2019). At the same time, the uncertainty of ground truth labels in real-world data may also affect the reliability of the systems. Particularly, in the medical domain, inter-rater variability is commonly observed despite the annotators' expertise (Sasada et al.,

2018; Jensen et al., 2019). This variability is also worth predicting for downstream tasks such as finding examples that need medical second opinions (Raghu et al., 2018).

To enhance the reliability of class probability estimates (CPEs), *post-hoc* calibration, which transforms output scores to fit into empirical class probabilities, has been proposed for both general classifiers (Platt et al., 1999; Zadrozny and Elkan, 2001, 2002) and neural networks (Guo et al., 2017; Kull et al., 2019). However, current evaluation metrics for calibration rely on empirical accuracy calculated with ground truth, for which the uncertainty of labels has not been considered. Another problem is that label uncertainty is not fully accounted for by CPEs; *e.g.*, a 50% confidence for class x does not necessarily mean the same amount of human belief, even when the CPEs are calibrated. Raghu et al. (2018) indicated that label uncertainty measures, such as an inter-rater disagreement frequency, were biased when they were estimated with CPEs. They instead proposed directly discriminating high uncertainty instances with input features. This treatment, however, requires training an additional predictor for each uncertainty measure and lacks an integrated view with the classification task.

In this work, we first develop an evaluation framework for CPEs when label uncertainty is indirectly observed through multiple annotations per instance (called *label histograms*). Guided with proper scoring rules (Gneiting and Raftery, 2007) and their decompositions (DeGroot and Fienberg, 1983; Kull and Flach, 2015), evaluation metrics, including calibration error, are naturally extensible to the situation with label histograms, where we derive estimators that benefit from unbiased or debiased property. Next, we generalize the framework to evaluate probabilistic predictions on higher-order statistics, including inter-rater disagreement. This extension enables us to evaluate these statistics in a unified way with CPEs. Finally, we address how the reliability of CPEs and disagreement probability estimates (DPEs) can be improved

using label histograms. While the existing post-hoc calibration methods solely address CPEs, we discuss the importance of obtaining a good predictive distribution over CPEs beyond point estimation to improve DPEs. Also, the distribution is expected to be useful for obtaining posterior CPEs when expert labels are provided for prediction. With these insights, we propose a novel method named α -calibration that uses label histograms to equip a neural network classifier with the ability to predict distributions of CPEs. In our experiments, the utility of our evaluation framework and α -calibration is demonstrated with synthetic data and a large-scale medical image dataset with multiple annotations provided from a study of myelodysplastic syndrome (MDS) (Sasada et al., 2018). Notably, α -calibration significantly enhances the quality of DPEs and the posterior CPEs.

In summary, our contributions are threefold as follows:

- Under ground truth label uncertainty, we develop evaluation metrics that benefit from unbiased or debiased property for class probability estimates (CPEs) using multiple labels per instance, *i.e.*, label histograms (Section 3).
- We generalize our framework to evaluate probability predictions on higher-order statistics, including inter-rater disagreement (Section 4).
- We advocate the importance of predicting the distributional uncertainty of CPEs, addressing with a newly devised post-hoc method, α -calibration (Section 5). Our approach substantially improves disagreement probability estimates (DPEs) and posterior CPEs for synthetic and real data experiments (Fig. 1 and Section 7).

2 Background

We overview calibration measures, proper scoring rules, and post-hoc calibration of CPEs as a prerequisite for our work.

Notation Let $K \in \mathbb{N}$ be a number of categories, $e^K = \{e_1, \dots, e_K\}$ be a set of K dimensional one-hot vectors (*i.e.*, $e_{kl} := \mathbb{I}[k = l]$), and $\Delta^{K-1} := \{\zeta \in \mathbb{R}_{\geq 0}^K : \sum_k \zeta_k = 1\}$ be a $K - 1$ -dimensional probability simplex. Let (X, Y) be jointly distributed random variables over \mathcal{X} and e^K , where X denotes an input feature, such as image data, and Y denotes a K -way label. Let $Z = (Z_1, \dots, Z_K)^\top := f(X) \in \Delta^{K-1}$ denote a random variable that represents class probability estimates (CPEs) for input X with a classifier $f : \mathcal{X} \rightarrow \Delta^{K-1}$.

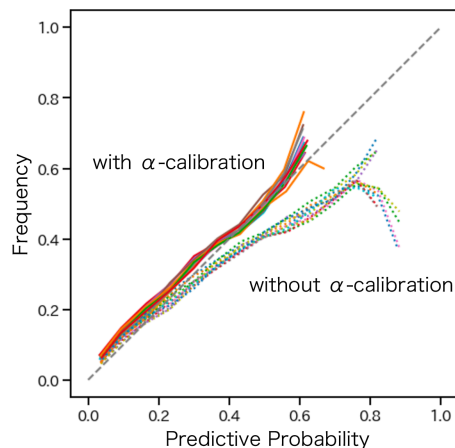


Figure 1: Reliability diagram of disagreement probability estimates (DPEs) in experiments with MDS data: a medical image dataset with multiple labels per instance. The dashed diagonal line corresponds to perfectly calibrated predictions. Calibrations of DPEs were significantly enhanced with α -calibration (solid lines) from the original ones (dotted lines).

2.1 Calibration measures

The notion of calibration, which is the agreement between a predictive class probability and an empirical class frequency, is important for reliable predictions. We reference Bröcker (2009); Kull and Flach (2015) for the definition of calibration.

Definition 1 (Calibration). ¹ A probabilistic classifier $f : \mathcal{X} \rightarrow \Delta^{K-1}$ is said to be calibrated if $Z = f(X)$ matches a true class probability given Z , *i.e.*, $\forall k, Z_k = C_k$, where $C_k := P(Y = e_k | Z)$ and $C := (C_1, \dots, C_K)^\top \in \Delta^{K-1}$, which we call a calibration map.

The following metric is commonly used to measure calibration errors of binary classifiers:

Definition 2 (Calibration error).

$$\text{CE}_1 := (\mathbb{E}[|Z_1 - C_1|^p])^{1/p}, \quad \text{where } p \geq 1. \quad (1)$$

Note that CE_1 takes the minimum value zero iff $Z = C$. The cases with $p = 1$ and 2 are called the expectation calibration error (ECE) (Naeini et al., 2015) and the squared calibration error (Kumar et al., 2019), respectively. Hereafter, we use $p = 2$ and let CE denote CE_1 for binary cases. For multiclass cases, we denote CE as a commonly used definition of class-wise calibration error (Kumar et al., 2019), *i.e.*, $(\sum_k \text{CE}_k^2)^{1/2}$.

¹A stronger notion of calibration that requires $Z = C$ is examined in the literature (Vaicenavicius et al., 2019; Widmann et al., 2019).

2.2 Proper scoring rules

Although calibration is a desirable property, being calibrated is not sufficient for useful predictions. For instance, a predictor that always presents the marginal class frequency $Z = (P(Y = e_1), \dots, P(Y = e_K))^\top$ is perfectly calibrated, but it entirely lacks the sharpness of prediction for labels stratified with Z . In contrast, the strictly proper scoring rules (Gneiting and Raftery, 2007; Parmigiani and Inoue, 2009) elicit a predictor’s true belief for each instance and do not suffer from this problem.

Definition 3 (Proper scoring rules for classification). *A loss function $\ell : e^K \times \Delta^{K-1} \rightarrow \mathbb{R}$ is said to be proper if $\forall q \in \Delta^{K-1}$ and for all $z \in \Delta^{K-1}$ such that $z \neq q$,*

$$\mathbb{E}_{Y \sim \text{Cat}(q)}[\ell(Y, z)] \geq \mathbb{E}_{Y \sim \text{Cat}(q)}[\ell(Y, q)] \quad (2)$$

holds, where $\text{Cat}(\cdot)$ denotes a categorical distribution. If the strict inequality holds, ℓ is said to be strictly proper. Following the convention, we write $\ell(q, z) = \mathbb{E}_{Y \sim \text{Cat}(q)}[\ell(Y, z)]$ for $q \in \Delta^{K-1}$.

For a strictly proper loss ℓ , the divergence function $d(q, z) := \ell(q, z) - \ell(q, q)$ takes a non-negative value and is zero iff $z = q$, by definition. Squared loss $\ell_{\text{sq}}(y, z) := \|y - z\|^2$ and logarithmic loss $\ell_{\log}(y, z) := -\sum_k y_k \log z_k$ are the most well-known examples of strictly proper loss. For these cases, the divergence functions are given as $d_{\text{sq}}(q, z) = \ell_{\text{sq}}(q, z)$ and $d_{\log}(q, z) = D_{\text{KL}}(q, z)$, a.k.a. KL divergence, respectively.

Let $L := \mathbb{E}[d(Y, Z)] = \mathbb{E}[d(Y, f(X))]$ denote the expected loss, where the expectation is taken over a distribution $P(X, Y)$. As special cases of L ,

$$L_{\text{sq}'} := \mathbb{E}[\ell_{\text{sq}'}(Y, Z)] = \mathbb{E}[(Y_1 - Z_1)^2] \quad (K = 2), \quad (3)$$

$$L_{\text{sq}} := \mathbb{E}[\ell_{\text{sq}}(Y, Z)] = \mathbb{E}[\|Y - Z\|^2] \quad (K \geq 2), \quad (4)$$

are commonly used for binary and multiclass prediction, respectively, where $\ell_{\text{sq}'} := \frac{1}{2}\ell_{\text{sq}}$. When the expectations are taken over an empirical distribution $\hat{P}(X, Y)$, these are referred to as Brier score (BS)² and probability score (PS), respectively (Brier, 1950; Murphy, 1973).

Decomposition of proper losses The relation between the expected proper loss L and the calibration measures is clarified with a decomposition of L as follows (DeGroot and Fienberg, 1983):

$$L = \text{CL} + \text{RL}, \quad \text{where} \quad \begin{cases} \text{CL} := \mathbb{E}[d(C, Z)], & (\text{Calibration Loss}) \\ \text{RL} := \mathbb{E}[d(Y, C)]. & (\text{Refinement Loss}) \end{cases} \quad (5)$$

²While Brier (1950) originally introduced a multiclass loss that equals PS, we call BS as Brier score, following convention (Bröcker, 2012; Ferro and Fricker, 2012).

The CL term corresponds to an error of calibration because the term will be zero iff Z equals the calibration map $C = \mathbb{E}[Y|Z]$. Relations $\text{CL}_{\text{sq}'} = \text{CE}^2$ and $\text{CL}_{\text{sq}} = \text{CE}^2$ can be confirmed for binary and multiclass cases, respectively. Complementarily, the RL term shows a dispersion of labels Y given Z from its mean $\mathbb{E}[Y|Z]$ averaged over Z .

Under the assumption that labels follow an instance-wise categorical distribution as $Y|X \sim \text{Cat}(Q)$, where $Q(X) \in \Delta^{K-1}$, Kull and Flach (2015) further decompose L into the following terms:

$$L = \underbrace{\text{CL} + \text{GL}}_{\text{EL}} + \text{IL}, \quad \text{where} \quad \begin{cases} \text{EL} = \mathbb{E}[d(Q, Z)], & (\text{Epistemic Loss}) \\ \text{IL} = \mathbb{E}[d(Y, Q)], & (\text{Irreducible Loss}) \\ \text{GL} = \mathbb{E}[d(Q, C)]. & (\text{Grouping Loss}) \end{cases} \quad (6)$$

The EL term, which equals zero iff $Z = Q$, is a more direct measure for the optimality of the model than L . The IL term stemming from the randomness of observations is called *aleatoric uncertainty* in the literature (Der Kiureghian and Ditlevsen, 2009; Senge et al., 2014). We refer to Appendix A for details and proofs of the statements in this section.

2.3 Post-hoc calibration for deep neural network classifiers

For deep neural network (DNN) classifiers with the softmax activation, a post-hoc calibration of class probability estimates (CPEs) is commonly performed by optimizing a linear transformation of the last layer’s logit vector (Guo et al., 2017; Kull et al., 2019), which minimizes the negative log-likelihood (NLL) of validation data:

$$\text{NLL} = -\mathbb{E}_{X, Y \sim \hat{P}}[\log P_{\text{obs}}(Y|\tilde{f}(X))], \quad (7)$$

where $\hat{P}, \tilde{f} : \mathcal{X} \rightarrow \Delta^{K-1}$ and $P_{\text{obs}}(Y|Z) = \prod_k Z_k^{Y_k}$ denote an empirical data distribution, a transformed DNN function from f , and a likelihood model, respectively. More details are described in Appendix D.1. In particular, temperature scaling, which has a single parameter and keeps the maximum confidence class unchanged, was the most successful in confidence calibration. More recent research (Wenger et al., 2020; Zhang et al., 2020; Rahimi et al., 2020) has proposed nonlinear calibration maps with favorable properties, such as expressiveness, data-efficiency, and accuracy-preservation.

3 Evaluation of class probability estimates with label histograms

Now, we formalize evaluation metrics for class probability estimates (CPEs) using label histograms, where multiple labels per instance are observed. We assume that N input samples are obtained in an i.i.d. manner: $\{x_i\}_{i=1}^N \sim P(X)$, and for each instance i , label histogram $y_i \in \mathbb{Z}_{\geq 0}^K$ is obtained from n_i annotators in a conditionally i.i.d. manner, *i.e.*, $\{y_i^{(j)}\}_{j=1}^{n_i} | x_i \sim P(Y|X = x_i)$ and $y_i = \sum_{j=1}^{n_i} y_i^{(j)}$. A predictive class probability for the i -th instance is denoted by $z_i = f(x_i) \in \Delta^{K-1}$. In this section, we assume ℓ_{sq} as a proper loss ℓ and omit the subscript from terms: EL and CL for brevity. The proofs in this section are found in Appendix B.

3.1 Expected squared and epistemic loss

We first derive an unbiased estimator of the expected squared loss L_{sq} from label histograms.

Proposition 1 (Unbiased estimator of expected squared loss). *The following estimator of L_{sq} is unbiased.*

$$\widehat{L}_{\text{sq}} := \sum_{i=1}^N \frac{w_i}{W} \sum_{k=1}^K [(\widehat{\mu}_{ik} - z_{ik})^2 + \widehat{\mu}_{ik}(1 - \widehat{\mu}_{ik})], \quad (8)$$

where $\widehat{\mu}_{ik} := y_{ik}/n_i$, $w_i \geq 0$, and $W := \sum_{i=1}^N w_i$.

Note that an optimal weight vector w that minimizes the variance $\mathbb{V}[\widehat{L}_{\text{sq}}]$ would be $w = 1$ if the number of annotators n_i is constant for all instances. Otherwise, it depends on undetermined terms, as discussed in Appendix B. We use $w = 1$ as a standard choice, where \widehat{L}_{sq} coincides with the probability score PS when every instance has a single label.

In addition to letting \widehat{L}_{sq} have higher statistical power than single-labeled cases, label histograms also enable us to directly estimate the epistemic loss EL, which is a discrepancy measure from the optimal model. A plugin estimator of EL is obtained as

$$\widetilde{\text{EL}} := \frac{1}{N} \sum_i \sum_k (\widehat{\mu}_{ik} - z_{ik})^2, \quad (9)$$

which, however, turns out to be severely biased. We alternatively propose the following estimator of EL.

Proposition 2 (Unbiased estimator of EL). *The following estimator of EL is unbiased.*

$$\widehat{\text{EL}} := \widetilde{\text{EL}} - \frac{1}{N} \sum_i \sum_k \frac{1}{n_i - 1} \widehat{\mu}_{ik}(1 - \widehat{\mu}_{ik}). \quad (10)$$

Note that the second correction term implies that $\widehat{\text{EL}}$ can only be evaluated when more than one label per instance is available. The bias correction effect is significant for a small n_i , which is relevant to most of the medical applications.

3.2 Calibration loss

Relying on the connection between CL and CE, we focus on evaluating CL to measure calibration. The calibration loss is further decomposed into class-wise terms as follows:

$$\text{CL} = \sum_k \text{CL}_k, \quad (11)$$

where $\text{CL}_k := \mathbb{E}[(C_k - Z_k)^2] = \mathbb{E}[\mathbb{E}[(C_k - Z_k)^2 | Z_k]]$. Thus, the case of CL_k is sufficient for subsequent discussion. Note that a difficulty exists in estimating the conditional expectation for Z_k . We take a standard binning-based approach (Zadrozny and Elkan, 2001) to evaluate CL_k by stratifying with Z_k values. Specifically, Z_k is partitioned into B_k disjoint regions $\mathcal{B}_k = \{[\zeta_0 = 0, \zeta_1), [\zeta_1, \zeta_2), \dots, [\zeta_{B_k-1}, \zeta_{B_k} = 1]\}$, and CL_k is approximated as follows:

$$\begin{aligned} \text{CL}_k(\mathcal{B}_k) &:= \sum_{b=1}^{B_k} \text{CL}_{kb}(\mathcal{B}_k), \quad \text{where} \\ \begin{cases} \text{CL}_{kb}(\mathcal{B}_k) &:= \mathbb{E}[\mathbb{E}[(\bar{C}_{kb} - \bar{Z}_{kb})^2 | Z_k \in \mathcal{B}_{kb}]], \\ \bar{C}_{kb} &:= \mathbb{E}[Y_k | Z_k \in \mathcal{B}_{kb}], \\ \bar{Z}_{kb} &:= \mathbb{E}[Z_k | Z_k \in \mathcal{B}_{kb}], \end{cases} \end{aligned} \quad (12)$$

in which CL_k is further decomposed into the bin-wise components. A plugin estimator of CL_{kb} is derived as follows:

$$\widetilde{\text{CL}}_{kb}(\mathcal{B}_k) := \frac{|I_{kb}|}{N} (\bar{c}_{kb} - \bar{z}_{kb})^2, \quad (13)$$

where, $I_{kb} = \{i : z_{ik} \in \mathcal{B}_{kb}\}$, $\bar{c}_{kb} := \sum_{i \in I_{kb}} \widehat{\mu}_{ik} / |I_{kb}|$, $\bar{z}_{kb} := \sum_{i \in I_{kb}} z_{ik} / |I_{kb}|$, and $|I_{kb}|$ denotes the size of I_{kb} . We can again improve the estimator by debiasing as follows:

Proposition 3 (Debiased estimator of CL_{kb}). *The plugin estimator of CL_{kb} is debiased with the following estimator:*

$$\begin{aligned} \widehat{\text{CL}}_{kb}(\mathcal{B}_k) &:= \widetilde{\text{CL}}_{kb}(\mathcal{B}_k) - \frac{|I_{kb}|}{N} \frac{\bar{\sigma}_{kb}^2}{|I_{kb}| - 1}, \quad \text{where} \\ \bar{\sigma}_{kb}^2 &:= \frac{1}{|I_{kb}|} \sum_{i \in I_{kb}} \widehat{\mu}_{ik}^2 - \left(\frac{1}{|I_{kb}|} \sum_{i \in I_{kb}} \widehat{\mu}_{ik} \right)^2. \end{aligned} \quad (14)$$

Note that the correction term against $\widetilde{\text{CL}}_{kb}$ would inflate for small-sized bins with a high label variance $\bar{\sigma}_{kb}^2$. $\widehat{\text{CL}}_{kb}$ can also be computed for single-labeled data, *i.e.*,

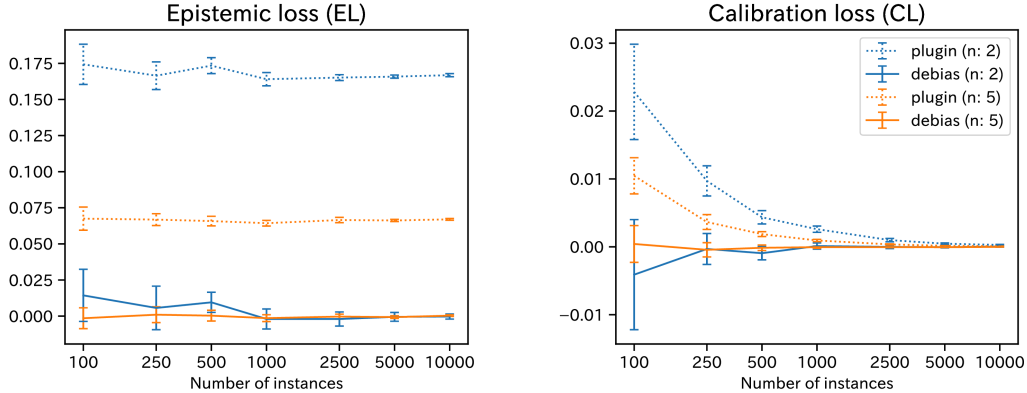


Figure 2: Comparison of the plugin and debiased estimators for synthetic data. For both EL and CL, the debiased estimators (solid lines) are closer to ground truth (which is zero in this experiment) than the plugin estimators (dotted lines). The error bars show 90% confidence intervals for the means of ten runs.

$\hat{\mu}_{ik} = y_{ik}$. In this case, the estimator precisely coincides with a debiased estimator for the *reliability* term formerly proposed in meteorological literature (Bröcker, 2012; Ferro and Fricker, 2012).

3.3 Debiasing effects of EL and CL estimators

To confirm the debiasing effect of estimators $\widehat{\text{EL}}$ and $\widehat{\text{CL}}$ against the plugin estimators, we experimented on evaluations of a perfect predictor using synthetic binary labels with varying instance sizes. For each instance, a positive label probability was drawn from a uniform distribution $U(0,1)$; thereby two or five labels were generated in an *i.i.d.* manner. The predictor indicated the true probabilities so that both EL and CL would be zero in expectation. As shown in Fig. 2, the debiased estimators significantly reduced the plugin estimators’ biases, even in the cases with two annotators. Details on the experimental setup are found in Appendix B.5.

4 Evaluation of higher-order statistics

Here, we generalize our framework to evaluate predictions on higher-order statistics. As is done for CPEs, the expected proper losses and calibration measures can also be formalized. We focus on a family of symmetric binary statistics $\phi : e^{K \times n} \rightarrow \{0, 1\}$ calculated from n distinct K -way labels for the same instance. For example, $\phi^{\text{D}} := \mathbb{I}[Y^{(1)} \neq Y^{(2)}]$ represents a disagreement between paired labels $(Y^{(1)}, Y^{(2)})$. The estimator of $\mathbb{E}[\phi^{\text{D}}|X]$ is known as the Gini-Simpson index, which is a measure of diversity.

Given a function $\varphi : \mathcal{X} \rightarrow [0, 1]$ that represents a predictive probability of being $\phi = 1$, the closeness of $\varphi(X)$ to a true probability $P(\phi = 1|X)$ is consistently evaluated with the expected (one dimensional) squared

loss $L_\phi := \mathbb{E}[(\phi - \varphi)^2]$. Then, the calibration loss CL_ϕ is derived by applying equation (5) as follows:

$$L_\phi = \underbrace{\mathbb{E}[(\mathbb{E}[\phi|\varphi] - \varphi)^2]}_{\text{CL}_\phi} + \underbrace{\mathbb{E}[(\phi - \mathbb{E}[\phi|\varphi])^2]}_{\text{RL}_\phi}. \quad (15)$$

An unbiased estimator of L_ϕ and a debiased estimator of CL_ϕ can be derived following a similar discussion as in CPEs. The biggest difference from the case of CPEs is that it requires more careful consideration to obtain an unbiased estimator of $\mu_{\phi,i} := \mathbb{E}[\phi|X = x_i]$ as follows:

$$\hat{\mu}_{\phi,i} := \binom{n_i}{n}^{-1} \sum_{j \in \text{Comb}(n_i, n)} \phi(y_i^{(j_1)}, \dots, y_i^{(j_n)}), \quad (16)$$

where $\text{Comb}(n_i, n)$ denotes the distinct subset of size n drawn from $\{1, \dots, n_i\}$ without replacement. The proof directly follows from the fact that $\hat{\mu}_{\phi,i}$ is a U-statistic of n -sample symmetric kernel function ϕ (Hoeffding et al., 1948). Details on the derivations for \widehat{L}_ϕ and $\widehat{\text{CL}}_\phi$ are described in Appendix C.

5 Post-hoc uncertainty calibration for DNNs with label histograms

We consider post-hoc uncertainty calibration problems using label histograms for a deep neural network (DNN) classifier f that offers CPE with the last layer’s softmax activation.

5.1 Class probability calibration

For post-hoc calibration of CPEs using label histograms, existing methods for single-labeled data (Section 2.3) are straightforwardly extensible by replacing the likelihood function P_{obs} in equation (7) with a multinomial distribution.

5.2 Importance of predicting distributional uncertainty of class probability estimates

Although we assume that labels for each input X are sampled from a categorical distribution $Q(X)$ in an i.i.d. manner, it is important to obtain a reliable CPE distribution beyond point estimation to perform several application tasks. We denote such a CPE distribution model as $P(\zeta|X)$, where $\zeta \in \Delta^{K-1}$. In this case, CPEs are written as $Z = \mathbb{E}[\zeta|X]$. Below, we illustrate two examples of those tasks.

Disagreement probability estimation For each input X , the extent of diagnostic disagreement among annotators is itself a signal worth predicting, which is different from classification uncertainty expressed as CPEs. Specifically, we aim at obtaining a disagreement probability estimation (DPE):

$$\varphi^D(X) = \int 1 - \sum_k \zeta_k^2 dP(\zeta|X) \quad (17)$$

as a reliable estimator of a probability $P(\phi^D = 1|X)$. When we only have CPEs, *i.e.*, $P(\zeta|X) = \delta(\zeta - f(X))$, where δ denotes the Dirac delta function, we get $\varphi^D = 1 - \sum_k f(X)_k^2$. However, $\varphi^D \simeq 0$ regardless of $f(X)$ would be more sensible if all the labels are given in unanimous.

Posterior class probability estimates We consider a task for updating CPEs of instance X after an expert’s annotation Y . Given a CPE distribution model $P(\zeta|X)$, an updated CPEs:

$$Z'(X, Y) := \mathbb{E}[\zeta|X, Y], \quad (18)$$

can be inferred from a Bayesian posterior computation: $P(\zeta|X, Y) \propto P(Y|\zeta)P(\zeta|X)$. If the prior distribution $P(\zeta|X)$ is reliable, Z' would be more close to the true value $Q(X)$ than the original CPEs Z in expectation.

5.3 α -calibration: post-hoc method for CPE distribution calibration

We propose a novel post-hoc calibration method called α -calibration that infers a CPE distribution $P(\zeta|X)$ from a DNN classifier f and validation label histograms. Specifically, we use a Dirichlet distribution $\text{Dir}(\zeta|\alpha_0(X)f(X))$ to model $P(\zeta|X)$, and minimize the NLL of label histograms with respect to instance-wise concentration parameter $\alpha_0(X) > 0$. We parameterize α_0 with a DNN that has a shared layer behind the last softmax activation of the DNN f and a successive full connection layer with an exp activation. Details are described in Appendix D.2. Using α_0 is one of the simplest ways to model the distribution over CPEs; hence it is computationally efficient and less

affected by over-fitting without crafted regularization terms. In addition, α -calibration has several favorable properties: it is orthogonally applicable with existing CPE calibration methods, will not degrade CPEs since $Z = \mathbb{E}[\zeta|X] = f(X)$ by design, and quantities of interest such as a DPE (17) and posterior CPEs (18) can be computed in closed forms as follows:

$$\varphi^D = \frac{\alpha_0}{\alpha_0 + 1} \left(1 - \sum_k f_k^2 \right), \quad Z' = \frac{\alpha_0 f + Y}{\alpha_0 + 1}. \quad (19)$$

Theoretical analysis We consider whether a CPE distribution model $P(\zeta|X) = \text{Dir}(\zeta|\alpha_0(X)f(X))$ is useful for downstream tasks. Let $G = g(X)$ denote a random variable of an output layer shared between both networks f and α_0 . We can write $P(\zeta|X) = P(\zeta|G)$ since f and α_0 are deterministic given G . Although it is unclear whether $P(\zeta|G)$ is an appropriate model for the true label distribution $P(Q|G)$, we can corroborate the utility of the model with the following analysis.

To evaluate the quality of DPEs and posterior CPEs dependent on α_0 , we analyze the expected loss $L_{\phi^D} = \mathbb{E}_G[L_{\phi^D, G}]$ and the epistemic loss $\text{EL}' := \mathbb{E}_G[\text{EL}'_G]$, respectively, where we define $L_{\phi^D, G} := \mathbb{E}[(\phi^D - \varphi^D)^2|G]$ and $\text{EL}'_G := \mathbb{E}[\sum_k (Z'_k - Q_k)^2|G]$. We denote those for the original model $P_0(\zeta|X) = \delta(\zeta - f(X))$ before α -calibration as $L_{\phi^D, G}^{(0)}$ and $\text{EL}'_G^{(0)}$, respectively.

Theorem 1. *There exist intervals for parameter $\alpha_0 \geq 0$, which improve task performances as follows.*

1. For DPEs, $L_{\phi^D, G} \leq L_{\phi^D, G}^{(0)}$ holds when $(1 - 2u_Q + s_Z)/2(u_Q - s_Z) \leq \alpha_0$, and $L_{\phi^D, G}$ takes the minimum value when $\alpha_0 = (1 - u_Q)/(u_Q - s_Z)$, if $u_Q > s_Z$ is satisfied.
2. For posterior CPEs, $\text{EL}'_G \leq \text{EL}'_G^{(0)}$ holds when $(1 - u_Q - \text{EL}_G)/2\text{EL}_G \leq \alpha_0$, and EL'_G takes the minimum value when $\alpha_0 = (1 - u_Q)/\text{EL}_G$, if $\text{EL}_G > 0$ is satisfied.

Note that we denote $s_Z := \sum_k Z_k^2$, $u_Q := \mathbb{E}[\sum_k Q_k^2|G]$, $v_Q := \mathbb{V}[Q_k|G]$, and $\text{EL}_G := \mathbb{E}[\sum_k (Z_k - Q_k)^2|G]$. The optimal α_0 of both tasks coincide to be $\alpha_0 = (1 - u_Q)/v_Q$, if CPEs match the true conditional class probabilities given G , *i.e.*, $Z = \mathbb{E}[Q|G]$.

The proof is shown in Appendix D.3.

6 Related work

Noisy labels Learning classifiers under label uncertainty has also been studied as a noisy label setting, assuming unobserved ground truth labels and label noises. The cases of uniform or class dependent noises

have been studied to ensure robust learning schemes (Natarajan et al., 2013; Jiang et al., 2018; Han et al., 2018) and predict potentially inconsistent labels (Northcutt et al., 2019). Also, there have been algorithms that modeled a generative process of noises depending on input features (Xiao et al., 2015; Liu et al., 2020). However, the paradigm of noisy labels requires qualified gold standard labels to validate predictions, while we assume that ground truth labels include uncertainty.

Multiple annotations Learning from multiple annotations per instance has also been studied in crowd-sourcing field (Guan et al., 2017; Rodrigues and Pereira, 2017; Tanno et al., 2019), which particularly modeled labelers with heterogeneous skills, occasionally including non-experts. In contrast, we focus on instance-wise uncertainty under homogeneous expertise as in Raghu et al. (2018). Another related paradigm is label distribution learning (Geng, 2016; Gao et al., 2017), which assumes instance-wise categorical probability as ground truth. Whereas they regard the true probability as observable, we assume it as a hidden variable on which actual labels depend.

Uncertainty of CPEs Approaches for predicting distributional uncertainty of CPEs for DNNs have mainly studied as part of Bayesian modeling. Gal and Ghahramani (2016); Lakshminarayanan et al. (2017); Teye et al. (2018); Wang et al. (2019) found practical connections for using ensembled DNN predictions as approximate Bayesian inference and uncertainty quantification (Kendall and Gal, 2017), which however require additional computational cost for sampling. An alternative approach is directly modeling CPE distribution with parametric families. In particular, Sensoy et al. (2018); Malinin and Gales (2018); Sadowski and Baldi (2018); Joo et al. (2020) adopted the Dirichlet distribution for a tractable distribution model and used for applications, such as detecting out-of-distribution examples. However, the use of multiple labels have not been explored in these studies. Moreover, these approaches need customized training procedures from scratch and are not designed to apply for DNN classifiers in a post-hoc manner, as is done in α -calibration.

7 Experiments

We applied DNN classifiers and calibration methods to synthetic and real-world image data with label histograms, where the performance was evaluated with our proposed metrics. Especially, we demonstrate the utility of α -calibration in two applications: predictions on inter-rater label disagreement (DPEs) and posterior CPEs, which we introduced in Section 5.2. Our

implementation is available online ³.

7.1 Experimental setup

Synthetic data We generated two synthetic image dataset: Mix-MNIST and Mix-CIFAR-10 from MNIST (LeCun et al., 2010) and CIFAR-10 (Krizhevsky et al., 2009), respectively. We randomly selected half of the images to create mixed-up images from pairs and the other half were retained as original. For each of the paired images, a random ratio that followed a uniform distribution $U(0, 1)$ was used for the mix-up and a class probability of multiple labels, which were two or five in validation set.

MDS data We used a large-scale medical imaging dataset for myelodysplastic syndrome (MDS) (Sasada et al., 2018), which contained over 90 thousand hematopoietic cell images obtained from blood specimens from 499 patients with MDS. This study was carried out in collaboration with medical technologists who mainly belonged to the Kyushu regional department of the Japanese Society for Laboratory Hematology. The use of peripheral blood smear samples for this study was approved by the ethics committee at Kumamoto University, and the study was performed in accordance with the Declaration of Helsinki. For each of the cellular images, a mean of 5.67 medical technologists annotated the cellular category from 22 subtypes, where accurate classification according to the current standard criterion was still challenging for technologists with expertise.

Compared methods We used DNN classifiers as base predictors (Raw) for CPEs, where a three layered CNN architecture for Mix-MNIST and a VGG16-based one for Mixed-CIFAR-10 and MDS were used. For CPE calibration, we adopted temperature scaling (ts), which was widely used for DNNs (Guo et al., 2017). To predict CPE distributions, we used α -calibration and ensemble-based methods: Monte-Carlo dropout (MCDO) (Gal and Ghahramani, 2016) and test-time augmentation (TTA) (Ayhan and Berens, 2018), which were both applicable to DNNs at prediction-time. Note that TTA was only applied for Mix-CIFAR-10 and MDS, in which we used data augmentation while training. We also combined ts and/or α -calibration with the ensemble-based methods in our experiments, while some of their properties, including the invariance of accuracy for ts and that of CPEs for α -calibration, were not retained for these combinations. The details of the network architectures and parameters were described in Appendix F.1. Considering a constraint of the high labeling costs with experts in the medical domain, we

³https://github.com/mim0r1/1h_calib

focused on scenarios that training instances were singly labeled and multiple labels were only available for the validation and test set.

7.2 Results

Class probability estimates We observed a superior performance of TTA in accuracy and \widehat{EL} and a consistent improvement in \widehat{EL} and \widehat{CL} with ts, for all the dataset. The details are found in Appendix F.1. By using \widehat{EL} , the relative performance of CPE predictions had been clearer than \widehat{L} since the irreducible loss was subtracted from \widehat{L} . We include additional MDS experiments using full labels in Appendix F.3, which show similar tendencies but improved overall performance.

Disagreement probability estimates We compared squared loss and calibration error of DPEs for combinations of prediction schemes (Table 1⁴). Notably, α -calibration combined with any methods showed a consistent and significant decrease in both \widehat{L}_{ϕ^D} and \widehat{CE}_{ϕ^D} , in contrast to MCDO and TTA, which had not solely improved the metrics. The improved calibration was also visually confirmed with a reliability diagram of DPEs for MDS data (Fig. 1).

Posterior CPEs We evaluated posterior CPEs, when one expert label per instance was available for test set. This task required a reasonable prior CPE model to update belief with additional label information. We summarize \widehat{EL} metrics of prior and posterior CPEs for combinations of dataset and prediction methods in Table 2. As we expected, α -calibration significantly decreased losses of the posterior CPEs, i.e., they got closer to the ideal CPEs than the prior CPEs. While TTA showed superior performance for the prior CPEs, the utility of the ensemble-based methods for the posterior computation was limited. We omit experiments on MCDO and TTA combined with α -calibration, as they require further approximation to compute posteriors.

8 Conclusion

In this work, we have developed a framework for evaluating probabilistic classifiers under ground truth label uncertainty, accompanied with useful metrics that benefited from unbiased or debiased properties. The framework was also generalized to evaluate higher-order statistics, including inter-rater disagreements. As a reliable distribution over class probability estimates (CPEs) is essential for higher-order prediction tasks, such as disagreement probability estimates (DPEs) and

posterior CPEs, we have devised a post-hoc calibration method called α -calibration, which directly used multiple annotations to improve CPE distributions. Throughout empirical experiments with synthetic and real-world medical image data, we have demonstrated the utility of the evaluation metrics in performance comparisons and a substantial improvement in DPEs and posterior CPEs with α -calibration.

Acknowledgements

IS was supported by JSPS KAKENHI Grant Number 20H04239 Japan. This work was supported by RAIDEN computing system at RIKEN AIP center.

References

- Murat Seekin Ayhan and Philipp Berens. Test-time data augmentation for estimation of heteroscedastic aleatoric uncertainty in deep neural networks. 2018.
- Glenn W Brier. Verification of forecasts expressed in terms of probability. *Monthly weather review*, 78(1): 1–3, 1950.
- Jochen Bröcker. Reliability, sufficiency, and the decomposition of proper scores. *Quarterly Journal of the Royal Meteorological Society: A journal of the atmospheric sciences, applied meteorology and physical oceanography*, 135(643):1512–1519, 2009.
- Jochen Bröcker. Estimating reliability and resolution of probability forecasts through decomposition of the empirical score. *Climate dynamics*, 39(3-4):655–667, 2012.
- François Chollet et al. Keras. <https://keras.io>, 2015.
- Morris H DeGroot and Stephen E Fienberg. The comparison and evaluation of forecasters. *Journal of the Royal Statistical Society: Series D (The Statistician)*, 32(1-2):12–22, 1983.
- Armen Der Kiureghian and Ove Ditlevsen. Aleatory or epistemic? does it matter? *Structural safety*, 31(2):105–112, 2009.
- Christopher AT Ferro and Thomas E Fricker. A bias-corrected decomposition of the brier score. *Quarterly Journal of the Royal Meteorological Society*, 138(668): 1954–1960, 2012.
- Yarin Gal and Zoubin Ghahramani. Dropout as a bayesian approximation: Representing model uncertainty in deep learning. In *international conference on machine learning*, pages 1050–1059, 2016.
- Bin-Bin Gao, Chao Xing, Chen-Wei Xie, Jianxin Wu, and Xin Geng. Deep label distribution learning with label ambiguity. *IEEE Transactions on Image Processing*, 26(6):2825–2838, 2017.

⁴The mechanisms that cause the degradation of DPEs for Raw+ts are discussed in Appendix F.2.

Table 1: Evaluations of disagreement probability estimates (DPEs)

Method	Mix-MNIST(2)		Mix-MNIST(5)		Mix-CIFAR-10(2)		Mix-CIFAR-10(5)		MDS	
	\widehat{L}_{ϕ^D}	\widehat{CE}_{ϕ^D}	\widehat{L}_{ϕ^D}	\widehat{CE}_{ϕ^D}	\widehat{L}_{ϕ^D}	\widehat{CE}_{ϕ^D}	\widehat{L}_{ϕ^D}	\widehat{CE}_{ϕ^D}	\widehat{L}_{ϕ^D}	\widehat{CE}_{ϕ^D}
Raw	.0755	.0782	.0755	.0782	.1521	.2541	.1521	.2541	.1477	.0628
Raw+ α	.0724	.0524	.0724	.0531	.0880	.0357	.0877	.0322	.1454	.0406
Raw+ts	.0775	.0933	.0773	.0923	.1968	.3310	.1978	.3324	.1482	.0663
Raw+ts+ α	.0699	.0344	.0702	.0379	.0863	.0208	.0861	.0164	.1445	.0261
MCDO	.0749	.0728	.0749	.0728	.1518	.2539	.1518	.2539	.1470	.0562
MCDO+ α	.0700	.0277	.0700	.0285	.0873	.0275	.0870	.0241	.1450	.0346
MCDO+ts	.0805	.1062	.0802	.1049	.1996	.3353	.2002	.3362	.1479	.0635
MCDO+ts+ α	.0690	.0155	.0691	.0188	.0863	.0196	.0861	.0167	.1442	.0186
TTA	NA	NA	NA	NA	.1677	.2856	.1677	.2856	.1441	.0488
TTA+ α	NA	NA	NA	NA	.0860	.0245	.0857	.0231	.1428	.0334
TTA+ts	NA	NA	NA	NA	.2421	.3957	.2430	.3968	.1448	.0553
TTA+ts+ α	NA	NA	NA	NA	.0872	.0467	.0870	.0398	.1422	.0197

Table 2: Epistemic losses (\widehat{EL}) of prior and posterior class probability estimates (CPEs)

Method	Mix-MNIST(2)		Mix-MNIST(5)		Mix-CIFAR-10(2)		Mix-CIFAR-10(5)		MDS	
	Prior	Post.	Prior	Post.	Prior	Post.	Prior	Post.	Prior	Post.
Raw+ α	.0388	.0292	.0388	.0292	.2504	.0709	.2504	.0693	.0435	.0354
Raw+ts+ α	.0379	.0293	.0379	.0298	.2423	.0682	.2423	.0676	.0430	.0352
MCDO	.0395	.0391	.0395	.0391	.2473	.2471	.2473	.2471	.0437	.0440
MCDO+ts	.0410	.0406	.0404	.0400	.2428	.2425	.2431	.2428	.0435	.0438
TTA	NA	NA	NA	NA	<u>.2216</u>	.2184	<u>.2216</u>	.2184	.0378	.0382
TTA+ts	NA	NA	NA	NA	.2452	.2428	.2451	.2427	.0379	.0383

Xin Geng. Label distribution learning. *IEEE Transactions on Knowledge and Data Engineering*, 28(7):1734–1748, 2016.

Tilmann Gneiting and Adrian E Raftery. Strictly proper scoring rules, prediction, and estimation. *Journal of the American statistical Association*, 102(477):359–378, 2007.

Melody Y Guan, Varun Gulshan, Andrew M Dai, and Geoffrey E Hinton. Who said what: Modeling individual labelers improves classification. *arXiv preprint arXiv:1703.08774*, 2017.

Chuan Guo, Geoff Pleiss, Yu Sun, and Kilian Q Weinberger. On calibration of modern neural networks. In *Proceedings of the 34th International Conference on Machine Learning-Volume 70*, pages 1321–1330. JMLR. org, 2017.

Bo Han, Quanming Yao, Xingrui Yu, Gang Niu, Miao Xu, Weihua Hu, Ivor Tsang, and Masashi Sugiyama. Co-teaching: Robust training of deep neural networks with extremely noisy labels. In *Advances in*

neural information processing systems, pages 8527–8537, 2018.

Kaiming He, Xiangyu Zhang, Shaoqing Ren, and Jian Sun. Deep residual learning for image recognition. In *Proceedings of the IEEE conference on computer vision and pattern recognition*, pages 770–778, 2016.

Wassily Hoeffding et al. A class of statistics with asymptotically normal distribution. *The Annals of Mathematical Statistics*, 19(3):293–325, 1948.

Martin Holm Jensen, Dan Richter Jørgensen, Raluca Jalaboi, Mads Eiler Hansen, and Martin Aastrup Olsen. Improving uncertainty estimation in convolutional neural networks using inter-rater agreement. In *International Conference on Medical Image Computing and Computer-Assisted Intervention*, pages 540–548. Springer, 2019.

Lu Jiang, Zhengyuan Zhou, Thomas Leung, Li-Jia Li, and Li Fei-Fei. Mentornet: Learning data-driven curriculum for very deep neural networks on cor-

- rupted labels. In *International Conference on Machine Learning*, pages 2304–2313, 2018.
- Taejong Joo, Uijung Chung, and Min-Gwan Seo. Being bayesian about categorical probability. *arXiv preprint arXiv:2002.07965*, 2020.
- Alex Kendall and Yarin Gal. What uncertainties do we need in bayesian deep learning for computer vision? In *Advances in neural information processing systems*, pages 5574–5584, 2017.
- Diederik P Kingma and Jimmy Ba. Adam: A method for stochastic optimization. *arXiv preprint arXiv:1412.6980*, 2014.
- Alex Krizhevsky, Geoffrey Hinton, et al. Learning multiple layers of features from tiny images. 2009.
- Meelis Kull and Peter Flach. Novel decompositions of proper scoring rules for classification: Score adjustment as precursor to calibration. In *Joint European Conference on Machine Learning and Knowledge Discovery in Databases*, pages 68–85. Springer, 2015.
- Meelis Kull, Miquel Perello Nieto, Markus Kängsepp, Telmo Silva Filho, Hao Song, and Peter Flach. Beyond temperature scaling: Obtaining well-calibrated multi-class probabilities with dirichlet calibration. In *Advances in Neural Information Processing Systems*, pages 12295–12305, 2019.
- Ananya Kumar, Percy S Liang, and Tengyu Ma. Verified uncertainty calibration. In *Advances in Neural Information Processing Systems*, pages 3787–3798, 2019.
- Balaji Lakshminarayanan, Alexander Pritzel, and Charles Blundell. Simple and scalable predictive uncertainty estimation using deep ensembles. In *Advances in neural information processing systems*, pages 6402–6413, 2017.
- Yann LeCun, Corinna Cortes, and CJ Burges. Mnist handwritten digit database. *ATT Labs [Online]*. Available: <http://yann.lecun.com/exdb/mnist>, 2, 2010.
- Yushan Liu, Markus M Geipel, Christoph Tietz, and Florian Buettner. Timely: Improving labeling consistency in medical imaging for cell type classification. *arXiv preprint arXiv:2007.05307*, 2020.
- Andrey Malinin and Mark Gales. Predictive uncertainty estimation via prior networks. In *Advances in Neural Information Processing Systems*, pages 7047–7058, 2018.
- Allan H Murphy. A new vector partition of the probability score. *Journal of applied Meteorology*, 12(4): 595–600, 1973.
- Mahdi Pakdaman Naeini, Gregory Cooper, and Milos Hauskrecht. Obtaining well calibrated probabilities using bayesian binning. In *Twenty-Ninth AAAI Conference on Artificial Intelligence*, 2015.
- Nagarajan Natarajan, Inderjit S Dhillon, Pradeep K Ravikumar, and Ambuj Tewari. Learning with noisy labels. In *Advances in neural information processing systems*, pages 1196–1204, 2013.
- Curtis G Northcutt, Lu Jiang, and Isaac L Chuang. Confident learning: Estimating uncertainty in dataset labels. *arXiv preprint arXiv:1911.00068*, 2019.
- Giovanni Parmigiani and Lurdes Inoue. *Decision theory: Principles and approaches*, volume 812. John Wiley & Sons, 2009.
- John Platt et al. Probabilistic outputs for support vector machines and comparisons to regularized likelihood methods. *Advances in large margin classifiers*, 10(3):61–74, 1999.
- Maithra Raghu, Katy Blumer, Rory Sayres, Ziad Obermeyer, Robert Kleinberg, Sendhil Mullainathan, and Jon Kleinberg. Direct uncertainty prediction for medical second opinions. *arXiv preprint arXiv:1807.01771*, 2018.
- Amir Rahimi, Amirreza Shaban, Ching-An Cheng, Byron Boots, and Richard Hartley. Intra order-preserving functions for calibration of multi-class neural networks. *arXiv preprint arXiv:2003.06820*, 2020.
- Filipe Rodrigues and Francisco Pereira. Deep learning from crowds. *arXiv preprint arXiv:1709.01779*, 2017.
- Peter Sadowski and Pierre Baldi. Neural network regression with beta, dirichlet, and dirichlet-multinomial outputs. 2018.
- Keiko Sasada, Noriko Yamamoto, Hiroki Masuda, Yoko Tanaka, Ayako Ishihara, Yasushi Takamatsu, Yutaka Yatomi, Waichiro Katsuda, Issei Sato, Hirotaka Matsui, et al. Inter-observer variance and the need for standardization in the morphological classification of myelodysplastic syndrome. *Leukemia research*, 69: 54–59, 2018.
- Robin Senge, Stefan Bösner, Krzysztof Dembczyński, Jörg Haasenritter, Oliver Hirsch, Norbert Donner-Banzhoff, and Eyke Hüllermeier. Reliable classification: Learning classifiers that distinguish aleatoric and epistemic uncertainty. *Information Sciences*, 255:16–29, 2014.
- Murat Sensoy, Lance Kaplan, and Melih Kandemir. Evidential deep learning to quantify classification uncertainty. In *Advances in Neural Information Processing Systems*, pages 3179–3189, 2018.
- Karen Simonyan and Andrew Zisserman. Very deep convolutional networks for large-scale image recognition. *arXiv preprint arXiv:1409.1556*, 2014.

- David B Stephenson, Caio AS Coelho, and Ian T Jolliffe. Two extra components in the brier score decomposition. *Weather and Forecasting*, 23(4):752–757, 2008.
- Ryutaro Tanno, Ardavan Saeedi, Swami Sankaranarayanan, Daniel C Alexander, and Nathan Silberman. Learning from noisy labels by regularized estimation of annotator confusion. In *Proceedings of the IEEE Conference on Computer Vision and Pattern Recognition*, pages 11244–11253, 2019.
- Mattias Teye, Hossein Azizpour, and Kevin Smith. Bayesian uncertainty estimation for batch normalized deep networks. In *International Conference on Machine Learning*, pages 4907–4916, 2018.
- Juozas Vaicenavicius, David Widmann, Carl Andersson, Fredrik Lindsten, Jacob Roll, and Thomas B Schön. Evaluating model calibration in classification. *arXiv preprint arXiv:1902.06977*, 2019.
- Guotai Wang, Wenqi Li, Michael Aertsen, Jan Deprest, Sébastien Ourselin, and Tom Vercauteren. Aleatoric uncertainty estimation with test-time augmentation for medical image segmentation with convolutional neural networks. *Neurocomputing*, 338:34–45, 2019.
- Jonathan Wenger, Hedvig Kjellström, and Rudolph Triebel. Non-parametric calibration for classification. In *International Conference on Artificial Intelligence and Statistics*, pages 178–190. PMLR, 2020.
- David Widmann, Fredrik Lindsten, and Dave Zachariah. Calibration tests in multi-class classification: A unifying framework. In *Advances in Neural Information Processing Systems*, pages 12236–12246, 2019.
- Tong Xiao, Tian Xia, Yi Yang, Chang Huang, and Xiaogang Wang. Learning from massive noisy labeled data for image classification. In *Proceedings of the IEEE conference on computer vision and pattern recognition*, pages 2691–2699, 2015.
- Bianca Zadrozny and Charles Elkan. Obtaining calibrated probability estimates from decision trees and naive bayesian classifiers. In *Icml*, volume 1, pages 609–616. Citeseer, 2001.
- Bianca Zadrozny and Charles Elkan. Transforming classifier scores into accurate multiclass probability estimates. In *Proceedings of the eighth ACM SIGKDD international conference on Knowledge discovery and data mining*, pages 694–699, 2002.
- Jize Zhang, Bhavya Kailkhura, and T Han. Mix-n-match: Ensemble and compositional methods for uncertainty calibration in deep learning. *arXiv preprint arXiv:2003.07329*, 2020.

Diagnostic Uncertainty Calibration: Towards Reliable Machine Predictions in Medical Domain (Appendix)

A Background for proper loss decomposition

We describe the proofs for proper loss decompositions introduced in section 2.

A.1 Decomposition of proper losses and calibration

As we have described in section 2.2, the expected loss L can be decomposed as follows:

Theorem 2 (DeGroot and Fienberg (1983)). *The expectation of proper loss ℓ is decomposed into non-negative terms as follows:*

$$L = \text{CL} + \text{RL}, \quad \text{where} \quad \begin{cases} \text{CL} := \mathbb{E}[d(C, Z)], & (\text{Calibration Loss}) \\ \text{RL} := \mathbb{E}[d(Y, C)], & (\text{Refinement Loss}) \end{cases} \quad (20)$$

where a calibration map $C := \mathbb{E}[Y|Z] \in \Delta^{K-1}$ is defined as in Def. 1.

Proof.

$$\begin{aligned} L &= \mathbb{E}[d(Y, Z)] \\ &= \mathbb{E}[\ell(Y, Z) - \ell(Y, Y)] \\ &= \mathbb{E}[\ell(Y, Z) - \ell(Y, C)] + \mathbb{E}[\ell(Y, C) - \ell(Y, Y)] \\ &= \mathbb{E}[\mathbb{E}[\ell(Y, Z) - \ell(Y, C)|Z]] + \mathbb{E}[d(Y, C)], \end{aligned}$$

where the second term equals to the RL term. For the first term, as we have defined $\ell(q, Z) := \mathbb{E}_{Y \sim \text{Cat}(q)}[\ell(Y, Z)]$ when $q \in \Delta^{K-1}$, the subterms can be rewritten as follows:

$$\begin{aligned} \mathbb{E}[\ell(Y, Z)|Z] &= \mathbb{E}_{Y \sim \text{Cat}(\mathbb{E}[Y|Z])}[\ell(Y, Z)] = \ell(\mathbb{E}[Y|Z], Z) = \ell(C, Z), \\ \mathbb{E}[\ell(Y, C)|Z] &= \mathbb{E}_{Y \sim \text{Cat}(\mathbb{E}[Y|Z])}[\ell(Y, C)] = \ell(\mathbb{E}[Y|Z], C) = \ell(C, C). \end{aligned}$$

Hence, the first term equals to the CL term as follows:

$$\mathbb{E}[\mathbb{E}[\ell(Y, Z) - \ell(Y, C)|Z]] = \mathbb{E}[\mathbb{E}[\ell(C, Z) - \ell(C, C)|Z]] = \mathbb{E}[d(C, Z)].$$

□

Note that we have followed the terminology used in Kull and Flach (2015). The terms CL and RL are also referred to as reliability (Bröcker, 2012; Ferro and Fricker, 2012) and sharpness (DeGroot and Fienberg, 1983).

A.2 Decomposition of proper losses under label uncertainty

As we have described in section 2.2, if Y follows an instance-wise categorical distribution with a probability vector, *i.e.*, $Y|X \sim \text{Cat}(Q)$, where $Q(X) \in \Delta^{K-1}$, L can be further decomposed as follows:

Theorem 3 (Kull and Flach (2015)). *The expectation of proper loss ℓ is decomposed into non-negative terms as follows:*

$$L = \text{EL} + \text{IL} = \underbrace{\text{CL} + \text{GL}}_{\text{EL}} + \text{IL}, \quad (21)$$

$$\text{where } \begin{cases} \text{EL} = \mathbb{E}[d(Q, Z)], & (\text{Epistemic Loss}) \\ \text{IL} = \mathbb{E}[d(Y, Q)], & (\text{Irreducible Loss}) \\ \text{GL} = \mathbb{E}[d(Q, C)]. & (\text{Grouping Loss}) \end{cases} \quad (22)$$

Note that the CL term is the same form as in equation (5).

Proof. We first prove the first equality.

$$\begin{aligned} L &= \mathbb{E}[d(Y, Z)] \\ &= \mathbb{E}[\ell(Y, Z) - \ell(Y, Y)] \\ &= \mathbb{E}[\ell(Y, Z) - \ell(Y, Q)] + \mathbb{E}[\ell(Y, Q) - \ell(Y, Y)] \\ &= \mathbb{E}[\mathbb{E}[\ell(Y, Z) - \ell(Y, Q)|Q]] + \mathbb{E}[d(Y, Q)], \end{aligned}$$

where the second term is IL. As similar to the proof of Theorem 2, the following relations hold:

$$\begin{aligned} \mathbb{E}[\ell(Y, Z)|Q] &= \mathbb{E}_{Y \sim Q}[\ell(Y, Z)|Q] = \mathbb{E}[\ell(Q, Z)|Q], \\ \mathbb{E}[\ell(Y, Q)|Q] &= \mathbb{E}_{Y \sim Q}[\ell(Y, Q)|Q] = \mathbb{E}[\ell(Q, Q)|Q]. \end{aligned}$$

Therefore, the first term turns out to be EL as follows:

$$\mathbb{E}[\mathbb{E}[\ell(Y, Z) - \ell(Y, Q)|Q]] = \mathbb{E}[\mathbb{E}[\ell(Q, Z) - \ell(Q, Q)|Q]] = \mathbb{E}[d(Q, Z)].$$

This term is further decomposed as follows:

$$\begin{aligned} \mathbb{E}[d(Q, Z)] &= \mathbb{E}[\ell(Q, Z) - \ell(Q, C)] + \mathbb{E}[\ell(Q, C) - \ell(Q, Q)] \\ &= \mathbb{E}[\mathbb{E}[\ell(Q, Z) - \ell(Q, C)|Z]] + \mathbb{E}[d(Q, C)], \end{aligned}$$

where the second term is GL. To show that the first term is CL, we have to prove the following results:

$$\begin{aligned} \mathbb{E}[\ell(Q, Z)|Z] &= \mathbb{E}[\ell(C, Z)|Z], \\ \mathbb{E}[\ell(Q, C)|Z] &= \mathbb{E}[\ell(C, C)|Z]. \end{aligned}$$

As these are proven with the same procedure, we only show the proof for the first equality.

$$\begin{aligned} \mathbb{E}[\ell(Q, Z)|Z] &= \mathbb{E}[\mathbb{E}_{Y \sim Q} \ell(Y, Z)|Z] \\ &= \mathbb{E}[\sum_k \ell(Y_k, Z) Q_k | Z] \\ &= \mathbb{E}[\sum_k \ell(Y_k, Z) \mathbb{E}[Y|Z]_k | Z] \\ &= \mathbb{E}[\sum_k \ell(Y_k, Z) C_k | Z] \\ &= \mathbb{E}[\mathbb{E}_{Y \sim C} \ell(Y, Z)|Z] = \mathbb{E}[\ell(C, Z)|Z]. \end{aligned}$$

□

Theorems and proofs for more generalized decompositions are found in Kull and Flach (2015).

B Details on CPE evaluation metrics with label histograms

We describe supplementary information for Section 3: proofs for propositions, additional discussion, and experimental setup.

B.1 Unbiased Estimators of L_{sq}

We give a proof for Prop. 1.

Restatement of Proposition 1 (Unbiased estimator of expected squared loss). *The following estimator of L_{sq} is unbiased.*

$$\widehat{L}_{\text{sq}} := \frac{1}{W} \sum_{i=1}^N w_i \sum_{k=1}^K [(\widehat{\mu}_{ik} - z_{ik})^2 + \widehat{\mu}_{ik}(1 - \widehat{\mu}_{ik})], \quad (23)$$

where $\widehat{\mu}_{ik} := y_{ik}/n_i$, $w_i \geq 0$, and $W := \sum_{i=1}^N w_i$.

Proof. We begin with the following plugin estimator of L_{sq} with an instance i :

$$\widetilde{L}_{\text{sq},i} := \sum_k \frac{1}{n_i} \sum_{j=1}^{n_i} (y_{ik}^{(j)} - z_{ik})^2. \quad (24)$$

By taking an expectation with respect to y_{ik} and z_{ik} ,

$$\mathbb{E}[\widetilde{L}_{\text{sq},i}] = \frac{1}{n_i} \sum_{j=1}^{n_i} \sum_k \mathbb{E}[(y_{ik}^{(j)} - z_{ik})^2] = \sum_k \mathbb{E}[(Y_k - Z_k)^2] = \mathbb{E}[\|Y - Z\|^2] = L_{\text{sq}}.$$

Therefore, $\widetilde{L}_{\text{sq},i}$ is an unbiased estimator of L_{sq} . Intuitively, an estimator combined with N instances is expected to have a lower variance than that with a single instance. A linear combination of $\widetilde{L}_{\text{sq},1}, \dots, \widetilde{L}_{\text{sq},N}$ is also an unbiased estimator as follows:

$$\frac{1}{W} \mathbb{E}[\sum_i w_i \widetilde{L}_{\text{sq},i}] = \frac{1}{W} \sum_i w_i \mathbb{E}[\widetilde{L}_{\text{sq},i}] = L_{\text{sq}},$$

where $\sum_i w_i \geq 0$, $W := \sum_i w_i$. The proof completes by transforming $\widetilde{L}_{\text{sq},i}$ as follows:

$$\widetilde{L}_{\text{sq},i} = \sum_k \frac{1}{n_i} \sum_{j=1}^{n_i} (y_{ik}^{(j)} - 2y_{ik}^{(j)} z_{ik} + z_{ik}^2) = \sum_k (\widehat{\mu}_{ik} - 2\widehat{\mu}_{ik} z_{ik} + z_{ik}^2) = \sum_k \widehat{\mu}_{ik}(1 - \widehat{\mu}_{ik}) + (\widehat{\mu}_{ik} - z_{ik})^2.$$

□

Determination of weights w For the undetermined weights w_1, \dots, w_N , we have argued that the optimal weights would be constant when the numbers of annotators n_1, \dots, n_N were constant. As we assume that each of an instance i follows an independent categorical distribution with a parameter $Q_i \in \Delta^{K-1}$, the variance of $\widehat{L}_{\text{sq},k}$ is decomposed as follows:

$$\mathbb{V}[\widehat{L}_{\text{sq},k}] = \sum_{i=1}^N \left(\frac{w_i}{W}\right)^2 \mathbb{V}[\widehat{L}_{\text{sq},i,k}]. \quad (25)$$

Thus, if n_i is constant for all the instance, the optimal weights are found as follows:

$$\min_{\mathbf{w}'} \sum_{i=1}^N w_i'^2 \quad s.t. \quad \sum_{i=1}^N w_i' = 1, \quad \forall i, w_i' \geq 0, \quad (26)$$

By taking a derivative with respect to \mathbf{w}' of $\sum_{i=1}^N w_i'^2 + \lambda(\sum_{i=1}^N w_i' - 1)$, the solution is $\forall i, w_i' = 1/N$.

For cases with varying numbers of annotators per instance, it is not straightforward to determine the optimal weights. From a standard result of variance formulas, the variance of \widehat{L}_{sq} is further decomposed as follows:

$$\begin{aligned}\mathbb{V}[\widehat{L}_{\text{sq},ik}] &:= \mathbb{E}[\mathbb{V}[\widehat{L}_{\text{sq},ik} | X_i]] + \mathbb{V}[\mathbb{E}[\widehat{L}_{\text{sq},ik} | X_i]] \\ &= \frac{1}{n_i} \mathbb{E}[\sigma_{\text{sq},k}^2(X)] + \mathbb{V}[\mu_{\text{sq},k}(X)],\end{aligned}$$

where $\mu_{\text{sq},k}(X) := \mathbb{E}[(Y_k - Z_k)^2 | X]$ and $\sigma_{\text{sq},k}^2(X) := \mathbb{V}[(Y_k - Z_k)^2 | X]$. Therefore, the optimal weights depend on the ratio of the first and the second terms. If the first term is negligible compared to the second term, using the constant weights regardless of n_i would be optimal. In contrast, if the first term is dominant, $w_i \propto n_i$ would be optimal. However, the ratio of the two terms depend on the dataset and is not determined a priori. In this work, we have used $w_i = 1$.

B.2 Unbiased Estimators of EL

In this section, we give a proof for Prop. 2.

Definition 4 (Plugin estimator of EL).

$$\widetilde{\text{EL}} := \frac{1}{N} \sum_{i=1}^N \sum_{k=1}^K (\widehat{\mu}_{ik} - z_{ik})^2. \quad (27)$$

Restatement of Proposition 2 (Unbiased estimator of EL). *The following estimator of EL is unbiased.*

$$\widehat{\text{EL}} := \widetilde{\text{EL}} - \frac{1}{N} \sum_i \sum_k \frac{1}{n_i - 1} \widehat{\mu}_{ik} (1 - \widehat{\mu}_{ik}). \quad (28)$$

Proof. The term EL is decomposed as $\text{EL} = \sum_k \text{EL}_k$, where

$$\text{EL}_k = \mathbb{E}[(Q_k - Z_k)^2] = \mathbb{E}[Q_k^2] - 2\mathbb{E}[Q_k Z_k] + \mathbb{E}[Z_k^2].$$

As for the terms in the plugin estimator $\widetilde{\text{EL}} = \sum_k \widetilde{\text{EL}}_k$, we can show that

$$\begin{aligned}\mathbb{E}[\widehat{\mu}_{ik} z_{ik}] &= \frac{1}{n_i} n_i \mathbb{E}[Q_k Z_k] = \mathbb{E}[Q_k Z_k], \\ \mathbb{E}[z_{ik}^2] &= \mathbb{E}[Z_k^2].\end{aligned}$$

The bias of $\widetilde{\text{EL}}_k$ comes from $\widehat{\mu}_{ik}^2$, that corresponds to $\mathbb{E}[Q_k^2]$ term. We can replace $\widehat{\mu}_{ik}^2$ by an unbiased estimator as follows:

$$\widehat{\mu}_{ik}^2 \rightarrow \frac{1}{n_i(n_i - 1)} \sum_{j=1}^{n_i} \sum_{j'=1: j' \neq j}^{n_i} y_{ik}^{(j)} y_{ik}^{(j')}, \quad (29)$$

where an expectation of each of the summand of *r.h.s.* is $\mathbb{E}[Q_k^2]$, hence that of *r.h.s.* is also be $\mathbb{E}[Q_k^2]$. Consequently, the difference of the plugin estimator $\widetilde{\text{EL}}_k$ and the unbiased estimator $\widehat{\text{EL}}_k$ is calculated as follows:

$$\begin{aligned}\widetilde{\text{EL}}_k - \widehat{\text{EL}}_k &= \frac{1}{N} \sum_i \left[\widehat{\mu}_i^2 - \frac{1}{n_i(n_i - 1)} \sum_{j=1}^{n_i} \sum_{j'=1: j' \neq j}^{n_i} y_{ik}^{(j)} y_{ik}^{(j')} \right] \\ &= \frac{1}{N} \sum_i \left\{ \widehat{\mu}_i^2 - \frac{1}{n_i(n_i - 1)} \left[\left(\sum_{j=1}^{n_i} y_{ik}^{(j)} \right)^2 - \sum_{j=1}^{n_i} y_{ik}^{(j)} \right] \right\} \\ &= \frac{1}{N} \sum_i \left\{ \widehat{\mu}_i^2 - \frac{1}{n_i(n_i - 1)} (n_i^2 \widehat{\mu}_{ik}^2 - n_i \widehat{\mu}_{ik}) \right\} \\ &= \frac{1}{N} \sum_i \frac{1}{n_i - 1} \widehat{\mu}_{ik} (1 - \widehat{\mu}_{ik}).\end{aligned}$$

□

B.3 Debiased Estimators of CL

In this section, we give a proof for Prop. 3.

Definition 5 (Plugin estimator of CL).

$$\widetilde{\text{CL}}_{kb}(\mathcal{B}_k) := \frac{|I_{kb}|}{N} (\bar{c}_{kb} - \bar{z}_{kb})^2, \quad \text{where } \bar{c}_{kb} := \frac{\sum_{i \in I_{kb}} \hat{\mu}_{ik}}{|I_{kb}|}, \quad \bar{z}_{kb} := \frac{\sum_{i \in I_{kb}} z_{ik}}{|I_{kb}|}, \quad (30)$$

where $I_{kb} := \{i \mid z_{ik} \in \mathcal{B}_k\}$ denotes an index set of b -th bin and $\mathcal{B}_k := [\zeta_{kb}, \zeta_{kb+1})$ is a b -th interval of the binning scheme \mathcal{B}_k .

Restatement of Proposition 3 (Debiased estimator of CL_{kb}). *The plugin estimator of CL_{kb} is debiased with the following estimator:*

$$\widehat{\text{CL}}_{kb}(\mathcal{B}_k) := \widetilde{\text{CL}}_{kb}(\mathcal{B}_k) - \frac{|I_{kb}|}{N} \frac{\bar{\sigma}_{kb}^2}{|I_{kb}| - 1}, \quad \text{where } \bar{\sigma}_{kb}^2 := \frac{1}{|I_{kb}|} \sum_{i \in I_{kb}} \hat{\mu}_{ik}^2 - \left(\frac{1}{|I_{kb}|} \sum_{i \in I_{kb}} \hat{\mu}_{ik} \right)^2. \quad (31)$$

Proof. The bias of the plugin estimator $\widetilde{\text{CL}}_{kb}$ is explained in a similar manner as in the case of $\widetilde{\text{EL}}_k$. Concretely, a bias of the term \bar{c}_{kb}^2 for an estimation of \bar{C}_{kb}^2 can be reduced with a following replacement:

$$\bar{c}_{kb}^2 \rightarrow \frac{1}{|I_{kb}| (|I_{kb}| - 1)} \sum_{i \in I_{kb}} \sum_{i' \in I_{kb}: i' \neq i} \hat{\mu}_{ik} \hat{\mu}_{i'k}. \quad (32)$$

Note that the *r.h.s.* term is only defined for the bin with $|I_{kb}| > 1$. In this case, a conditional expectation of the term is as follows:

$$\begin{aligned} \mathbb{E}\left[\frac{|I_{kb}|}{N} \cdot \text{r.h.s.}, |I_{kb}| > 1\right] &= \sum_{m=2}^N \frac{\mathbb{E}[|I_{kb}| = m] m}{N} \frac{1}{m(m-1)} \sum_{i \in I_{kb}} \sum_{i' \in I_{kb}: i' \neq i} \mathbb{E}[\hat{\mu}_{ik} \hat{\mu}_{i'k} \mid |I_{kb}| = m] \\ &= \sum_{m=2}^N \frac{\mathbb{E}[|I_{kb}| = m] m}{N} \bar{C}_{kb}^2 = \frac{\mathbb{E}[|I_{kb}| \mid |I_{kb}| > 1]}{N} \bar{C}_{kb}^2 \\ &= (\mathbb{E}[Z_k \in \mathcal{B}_k] - \eta_{kb}) \bar{C}_{kb}^2, \end{aligned}$$

where $\eta_{kb} = \mathbb{E}[|I_{kb}| \leq 1]/N$, which can be reduced by increasing N relative to the bin size. When we use the *r.h.s.* = 0 for $|I_{kb}| \leq 1$, $\eta_{kb} \bar{C}_{kb}^2$ is a remained bias term after the replacement in equation (32). When we define an estimator $\widehat{\text{CL}}_{kb}$ as a modified $\widetilde{\text{CL}}_{kb}$ that has been applied the replacement (32), a debiasing amount of the bias with the modification is calculated as follows:

$$\begin{aligned} \widetilde{\text{CL}}_{kb} - \widehat{\text{CL}}_{kb} &= \frac{|I_{kb}|}{N} \left\{ \bar{c}_{kb}^2 - \frac{1}{|I_{kb}| (|I_{kb}| - 1)} \sum_{i \in I_{kb}} \sum_{i' \in I_{kb}: i' \neq i} \hat{\mu}_{ik} \hat{\mu}_{i'k} \right\} \\ &= \frac{|I_{kb}|}{N} \left\{ \bar{c}_{kb}^2 - \frac{1}{|I_{kb}| (|I_{kb}| - 1)} \left[(|I_{kb}| \bar{c}_{kb})^2 - \sum_{i \in I_{kb}} \hat{\mu}_{ik}^2 \right] \right\} \\ &= \frac{|I_{kb}|}{N} \left\{ \frac{1}{|I_{kb}| - 1} \left[\frac{1}{|I_{kb}|} \sum_{i \in I_{kb}} \hat{\mu}_{ik}^2 - \bar{c}_{kb}^2 \right] \right\} = \frac{|I_{kb}|}{N} \frac{\bar{\sigma}_{kb}^2}{|I_{kb}| - 1}. \end{aligned}$$

□

Note that as we mentioned in the proof, the bin-wise debiasing cannot be applied for the bins with $|I_{kb}| \leq 1$. We use 0 for the estimators with such bins. For single-labeled data, the remaining bias from this limitation is also analyzed in the literature (Ferro and Fricker, 2012).

B.4 Definition and estimators of dispersion loss

We consider to estimate the remainder term $\text{EL} - \text{CL}$. As we present in equation (6), EL is decomposed into $\text{CL} + \text{GL}$, in which GL is a loss relating to the lack of predictive sharpness. However, the approximate calibration loss $\text{CL}(\mathcal{B})$ is known to be underestimated (Vaicenavicius et al., 2019; Kumar et al., 2019) in relation to the coarseness of the selected binning scheme \mathcal{B} . On the other hand, EL does not suffer from a resolution of \mathcal{B} . Instead of estimating the GL term for binned predictions with \mathcal{B} , we use the difference term $\text{DL}(\mathcal{B}) := \text{EL} - \text{CL}(\mathcal{B})$, which we call dispersion loss. The non-negativity of $\text{DL}(\mathcal{B})$ is shown as follows.

Proposition 4 (Non-negativity of dispersion loss). *Given a binning scheme \mathcal{B} , a dispersion loss for class k is decomposed into bin-wise components, where each term takes a non-negative value:*

$$\text{DL}_k(\mathcal{B}) := \text{EL}_k - \text{CL}_k(\mathcal{B}) = \sum_b \text{DL}_{kb}(\mathcal{B}), \quad (33)$$

$$\text{DL}_{kb}(\mathcal{B}) := \mathbb{E}[\mathbb{E}[\{(Q_k - \bar{C}_{kb}) - (Z_k - \bar{Z}_{kb})\}^2 | Z_k \in \mathcal{B}_{kb}]] \geq 0. \quad (34)$$

Proof. From the definition of $\text{DL}_k(\mathcal{B})$,

$$\begin{aligned} \text{DL}_k(\mathcal{B}) &:= \text{EL}_k - \text{CL}_k(\mathcal{B}) \\ &= \mathbb{E}[(Q_k - Z_k)^2] - \sum_b \mathbb{E}[\mathbb{E}[(\bar{C}_{kb} - \bar{Z}_{kb})^2 | Z_k \in \mathcal{B}_{kb}]] \\ &= \sum_b \mathbb{E}[\mathbb{E}[(Q_k - Z_k)^2 - (\bar{C}_{kb} - \bar{Z}_{kb})^2 | Z_k \in \mathcal{B}_{kb}]] \\ &= \sum_b \text{DL}_{kb}(\mathcal{B}), \\ &\quad \text{where } \text{DL}_{kb}(\mathcal{B}) := \mathbb{E}[\mathbb{E}[(Q_k - Z_k)^2 - (\bar{C}_{kb} - \bar{Z}_{kb})^2 | Z_k \in \mathcal{B}_{kb}]]. \end{aligned}$$

By noting that $\bar{C}_{kb} - \bar{Z}_{kb} = \mathbb{E}[Q_k - Z_k | Z_k \in \mathcal{B}_{kb}]$, the last term is further transformed as follows:

$$\begin{aligned} \text{DL}_{kb}(\mathcal{B}) &= \mathbb{E}[\mathbb{E}[(Q_k - Z_k)^2 - (\bar{C}_{kb} - \bar{Z}_{kb})^2 | Z_k \in \mathcal{B}_{kb}]] \\ &= \mathbb{E}[\mathbb{E}[(Q_k - Z_k)^2 - 2(Q_k - Z_k)(\bar{C}_{kb} - \bar{Z}_{kb}) + (\bar{C}_{kb} - \bar{Z}_{kb})^2 | Z_k \in \mathcal{B}_{kb}]] \\ &= \mathbb{E}[\mathbb{E}[\{(Q_k - Z_k) - (\bar{C}_{kb} - \bar{Z}_{kb})\}^2 | Z_k \in \mathcal{B}_{kb}]] \\ &= \mathbb{E}[\mathbb{E}[\{(Q_k - \bar{C}_{kb}) - (Z_k - \bar{Z}_{kb})\}^2 | Z_k \in \mathcal{B}_{kb}]]. \end{aligned}$$

Then, the last term is apparently ≥ 0 . \square

From equation (34), the DL term can be interpreted as the average of the bin-wise overdispersion of the true class probability Q_k , which is unaccounted for by the deviation of Z_k . For single-labeled cases, similar argument is found in (Stephenson et al., 2008). The plugin and debiased estimators of DL are derived from those of EL and CL , respectively.

By using the plugin and the debiased estimators of EL and CL , those estimators of DL are defined as follows:

Definition 6 (Plugin / debiased estimators of dispersion loss).

$$\widetilde{\text{DL}}_{kb}(\mathcal{B}) = \frac{1}{N} \sum_{i \in I_{kb}} \{(\hat{\mu}_{ik} - \bar{c}_{kb}) - (z_{ik} - \bar{z}_{kb})\}^2, \quad (35)$$

$$\widehat{\text{DL}}_{kb}(\mathcal{B}) = \widetilde{\text{DL}}_{kb}(\mathcal{B}) - \frac{1}{N} \sum_{i \in I_{kb}} \left(\frac{1}{n_i - 1} \hat{\mu}_{ik}(1 - \hat{\mu}_{ik}) - \frac{\bar{\sigma}_{kb}^2}{|I_{kb}| - 1} \right). \quad (36)$$

B.5 Experimental setup for debiasing effects of EL and CL terms

The details of the experimental setup for Section 3.3 are described. We experimented on evaluations of a perfect predictor that indicated correct instance-wise CPEs, using synthetic binary labels with varying instance sizes: from 100 to 10,000. For each instance, the positive probability for label generation was drawn from a uniform

distribution $U(0, 1)$, and two or five labels were generated in an i.i.d. manner following a Binomial distribution with the corresponding probability. Since the predictor indicated the correct probability, EL and CL would be zero in expectation. For a binning scheme \mathcal{B} of the estimators, we adopted 15 equally-spaced binning, which was regularly used to evaluate calibration errors (Guo et al., 2017).

C Details on higher-order statistics evaluation

The details and proofs for the statements in section 4 are described. Let $X \in \mathcal{X}$ be an input feature and $\{Y^{(j)} \in e^K\}_{j=1}^n$ be n distinct labels for the same instance. We define a symmetric categorical statistics $\phi : e^{K \times n} \rightarrow e^M (M \geq 2)$ for the n labels. For the case of $M = 2$, ϕ can be equivalently represented as $\phi : e^{K \times n} \rightarrow \{0, 1\}$, and we use this definition for the successive discussion. In our experiments, we particularly focus on a disagreement between paired labels $\phi^D = \mathbb{I}[Y^{(1)} \neq Y^{(2)}]$ as predictive target.

Consider a probability prediction $\varphi : \mathcal{X} \rightarrow [0, 1]$ for statistics $\phi : e^{K \times n} \rightarrow \{0, 1\}$, a strictly proper loss $\ell : \{0, 1\} \times [0, 1] \rightarrow \mathbb{R}$ encourages $\varphi(X)$ to approach the right probability $P(\phi(Y^{(1)}, \dots, Y^{(n)})|X)$ in expectation. We use (one dimensional) squared loss $\ell(\phi, \varphi) = (\phi - \varphi)^2$ in our evaluation. The expected loss is as follows:

Definition 7 (Expected squared loss for ϕ and φ).

$$L_\phi := \mathbb{E}[(\phi - \varphi)^2], \quad (37)$$

where the expectation is taken over the random variables X and $Y^{(1)}, \dots, Y^{(n)}$.

Note that L_ϕ for an empirical distribution is equivalent to Brier score of ϕ and φ . A decomposition of L_ϕ into CL_ϕ and RL_ϕ is readily available by applying Theorem 2.

$$L_\phi := \mathbb{E}[(\phi - \varphi)^2] = \underbrace{\mathbb{E}[(\mathbb{E}[\phi|\varphi] - \varphi)^2]}_{\text{CL}_\phi} + \underbrace{\mathbb{E}[(\phi - \mathbb{E}[\phi|\varphi])^2]}_{\text{RL}_\phi}. \quad (38)$$

We will derive the estimators of L_ϕ and CL_ϕ as evaluation metrics. However, the number of labels per instance is $n_i \geq n$ in general⁵, which results in multiple inconsistent statistics ϕ for the same instance. The problem can be solved with similar treatments as in the evaluation of CPEs.

As we stated in section 4, an unbiased estimator of the mean statistics for each instance $\mu_{\phi,i} := \mathbb{E}[\phi|X = x_i]$ is a useful building block in the estimation of L_ϕ and CL_ϕ . Recall that we assume a conditional independence of an arbitrary number of labels given an input feature, i.e., $Y^{(1)}, \dots, Y^{(n_i)}|X \underset{i.i.d.}{\sim} \text{Cat}(Q(X))$, $\mu_{\phi,i}$ is estimated as follows:

Theorem 4 (Unbiased estimator of $\mu_{\phi,i}$). *For an instance i with n_i labels obtained in a conditional i.i.d. manner, an unbiased estimator of the conditional mean $\mu_{\phi,i}$ is given as follows:*

$$\hat{\mu}_{\phi,i} := \binom{n_i}{n}^{-1} \sum_{j \in \text{Comb}(n_i, n)} \phi(y_i^{(j_1)}, \dots, y_i^{(j_n)}), \quad (39)$$

where $\text{Comb}(n_i, n)$ denotes the distinct subset of size n drawn from $\{1, \dots, n_i\}$ without replacement.

Proof. This is directly followed from the fact that $\hat{\mu}_{\phi,i}$ is a U-statistic of n -sample symmetric kernel function ϕ (Hoeffding et al., 1948). \square

C.1 Unbiased estimator of L_ϕ

We give an unbiased of L_ϕ as follows:

Theorem 5 (Unbiased estimator of L_ϕ). *The following estimator is an unbiased estimator of L_ϕ .*

$$\hat{L}_\phi := \frac{1}{N} \sum_i \hat{L}_{\phi,i}, \quad \text{where} \quad \hat{L}_{\phi,i} := \binom{n_i}{n}^{-1} \sum_{j \in \text{Comb}(n_i, n)} \left(\phi(y_i^{(j_1)}, \dots, y_i^{(j_n)}) - \varphi_i \right)^2. \quad (40)$$

⁵We omit an instance with $n_i < n$ where ϕ cannot be calculated with distinct n labels.

Proof. We first confirm that, for each random variables $\phi(y_i^{(1)}, \dots, y_i^{(n)})$ and φ_i of sample i ,

$$\mathbb{E}[f(y_i^{(1)}, \dots, y_i^{(n)}; \varphi_i)] = L_\phi, \quad \text{where} \quad f(y_i^{(1)}, \dots, y_i^{(n)}; \varphi_i) := \left(\phi(y_i^{(1)}, \dots, y_i^{(n)}) - \varphi_i \right)^2,$$

is satisfied by definition. As f is an n -sample symmetric kernel of variables $y_i^{(1)}, \dots, y_i^{(n)}$, $\widehat{L}_{\phi,i}$ is a U-statistic (Hoeffding et al., 1948) of the kernel given φ_i and also an unbiased estimator of L_ϕ as follows:

$$\mathbb{E}[\widehat{L}_{\phi,i}] = \mathbb{E}[\mathbb{E}[\widehat{L}_{\phi,i} | \varphi_i]] = \mathbb{E}[\mathbb{E}[f(y_i^{(1)}, \dots, y_i^{(n)}; \varphi_i) | \varphi_i]] = L_\phi. \quad (41)$$

Hence

$$\mathbb{E}[\widehat{L}_\phi] = \frac{1}{N} \sum_{i=1}^N \mathbb{E}[\widehat{L}_{\phi,i}] = L_\phi.$$

□

C.2 Debiased estimator of $\text{CL}_\phi(\mathcal{B})$

Following the same discussion as the $\text{CL}(\mathcal{B})$ term of CPEs, we also consider a binning based approximation of CL_ϕ stratified with a binning scheme \mathcal{B} for predictive probability $\varphi \in [0, 1]$. Then, the plugin estimator of $\text{CL}_\phi(\mathcal{B})$ is defined as follows:

Definition 8 (Plugin estimator of CL_ϕ).

$$\widetilde{\text{CL}}_\phi(\mathcal{B}) := \sum_{b=1}^B \widetilde{\text{CL}}_{\phi,b}(\mathcal{B}), \quad (42)$$

$$\text{where} \quad \widetilde{\text{CL}}_{\phi,b}(\mathcal{B}) := \frac{|I_{\phi,b}|}{N} (\bar{c}_{\phi,b} - \bar{\varphi}_b)^2, \quad \bar{c}_{\phi,b} := \frac{\sum_{i \in I_{\phi,b}} \widehat{\mu}_{\phi,i}}{|I_{\phi,b}|}, \quad \bar{\varphi}_b := \frac{\sum_{i \in I_{\phi,b}} \varphi_i}{|I_{\phi,b}|}. \quad (43)$$

We again improve the plugin estimator with the following debiased estimator $\widehat{\text{CL}}_{\phi,b}(\mathcal{B})$:

Corollary 6 (Debiased estimator of $\text{CL}_{\phi,b}$). *A plugin estimator $\widetilde{\text{CL}}_{\phi,b}(\mathcal{B})$ of $\text{CL}_{\phi,b}(\mathcal{B})$ is debiased to $\widehat{\text{CL}}_{\phi,b}(\mathcal{B})$ with a correction term as follows:*

$$\widehat{\text{CL}}_{\phi,b}(\mathcal{B}) := \widetilde{\text{CL}}_{\phi,b}(\mathcal{B}) - \frac{|I_{\phi,b}|}{N} \frac{\bar{\sigma}_{\phi,b}^2}{|I_{\phi,b}| - 1}, \quad (44)$$

$$\text{where} \quad \bar{\sigma}_{\phi,b}^2 := \frac{1}{|I_{\phi,b}|} \sum_{i \in I_{\phi,b}} \widehat{\mu}_{\phi,i}^2 - \left(\frac{1}{|I_{\phi,b}|} \sum_{i \in I_{\phi,b}} \widehat{\mu}_{\phi,i} \right)^2. \quad (45)$$

Note that the estimator is only available for bins with $|I_{\phi,b}| \geq 2$.

Proof. The proof follows a similar reasoning to Prop. B.3. We reduce the bias introduced with the term $\bar{c}_{\phi,b}^2$ by replacing the term with unbiased one for $\bar{C}_{\phi,b}^2 = \mathbb{E}[\phi | \varphi \in \mathcal{B}_b]^2$ as follows:

$$\bar{c}_{\phi,b}^2 \rightarrow \frac{1}{|I_{\phi,b}| (|I_{\phi,b}| - 1)} \sum_{i \in I_{\phi,b}} \sum_{i' \in I_{\phi,b}; i' \neq i} \widehat{\mu}_{\phi,i} \widehat{\mu}_{\phi,i'},$$

where $\widehat{\mu}_{\phi,i}$ is defined in equation (39). An improvement with the debiased estimator $\widetilde{\text{CL}}_{\phi,b} - \widehat{\text{CL}}_{\phi,b}$ is also calculated with the same manner as in Prop. B.3. □

C.3 Summary of evaluation metrics introduced for label histograms

In Table 3, we summarize evaluation metrics introduced for label histograms, where *order* shows the required numbers of labels for each instance to define the metrics, and *rater* represents those for estimating the metrics.

Table 3: Summary of evaluation metrics introduced for label histograms

Order	Signature	Description	Rater
1	$L_{\text{sq}} = \text{EL} + \text{IL}$	Expected squared loss of CPEs	≥ 1
	$\text{EL} = \text{CL} + \text{DL}$	Epistemic loss of CPEs	≥ 2
	$\text{CL} = \text{CE}^2$	Calibration loss of CPEs	≥ 1
	DL	Dispersion loss of CPEs	≥ 2
2	$L_{\phi^{\text{D}}}$	Expected squared loss of DPEs	≥ 2
	$\text{CL}_{\phi^{\text{D}}}$	Calibration loss of DPEs	≥ 2

D Details on post-hoc uncertainty calibration methods

D.1 CPE calibration methods based on linear transformations

To complement Section 2.3, we summarize the formulation of CPE (class probability estimation) calibration that is based on linear transformations. Let $x \in \mathcal{X}$ denotes an input data, $u : \mathcal{X} \rightarrow \mathbb{R}^K$ denotes a DNN function that outputs a logit vector, and $f(x) = \text{softmax}(u(x)) \in \Delta^{K-1}$ denotes CPEs. A common form of CPE calibration with linear transformations is given as follows:

$$\tilde{u}(x) = Wu(x) + b, \quad (46)$$

$$\tilde{f}(x) = \text{softmax}(\tilde{u}(x)), \quad (47)$$

where $\tilde{u}(x)$ denotes transformed logits with parameters $W \in \mathbb{R}^{K \times K}$ and $b \in \mathbb{R}^K$, and $\tilde{f} : \mathcal{X} \rightarrow \Delta^{K-1}$ denotes CPEs after calibration.

The most general form of equation (46) is referred to as matrix scaling (Guo et al., 2017; Kull et al., 2019). A version of that with a constraint $W = \text{diag}(v)$, $v \in \mathbb{R}^K$ and that with a further constraint $v = 1/t$, $t \in \mathbb{R}$, $b = 0$ are called vector and temperature scaling, respectively. In particular, temperature scaling has a favorable property; it does not change the maximum predictive class of each instance, and hence neither the overall accuracy, as the order of vector elements between u and \tilde{u} for each x is unchanged.

For vector and matrix scaling, regularization terms are required to prevent over-fitting; L2 regularization of b :

$$\Omega_{\text{L2}}(b) := \lambda_b \frac{1}{K} \sum_k b_k^2 \quad (48)$$

is commonly used for vector scaling, and off-diagonal and intercept regularization (ODIR):

$$\Omega_{\text{ODIR}}(W, b) := \lambda_w \frac{1}{K(K-1)} \sum_{k \neq k'} W_{kk'}^2 + \lambda_b \frac{1}{K} \sum_k b_k^2 \quad (49)$$

is proposed for matrix scaling, which is used for improving class-wise calibration (Kull et al., 2019).

D.2 Details on α -calibration

Loss function For the loss function for α -calibration, we use a variant of NLL in equation (7) as follows:

$$-\frac{1}{\sum_i n_i} \sum_i \log \text{DirMult}(y_i | \alpha_0(x_i) f(x_i)) + \frac{\lambda_\alpha}{N} \sum_i (\log \alpha_0(x_i))^2, \quad (50)$$

where $\text{DirMult}(\cdot)$ denotes the Dirichlet multinomial distribution, and a regularization term $\lambda_\alpha (\log \alpha_0)^2$ is introduced for stabilization purpose, which penalizes the deviation from $\alpha_0 = 1$ to both directions towards extreme concentrations of the mass: $P(\zeta|X) \rightarrow \delta(\zeta = f(X))$ with $\alpha_0 \rightarrow \infty$ or $P(\zeta|X) \rightarrow \sum_k \delta(\zeta = e_k) \mathbb{E}[\zeta_k]$ with $\alpha_0 \rightarrow 0$. We employ $\lambda_\alpha = 0.005$ throughout this study.

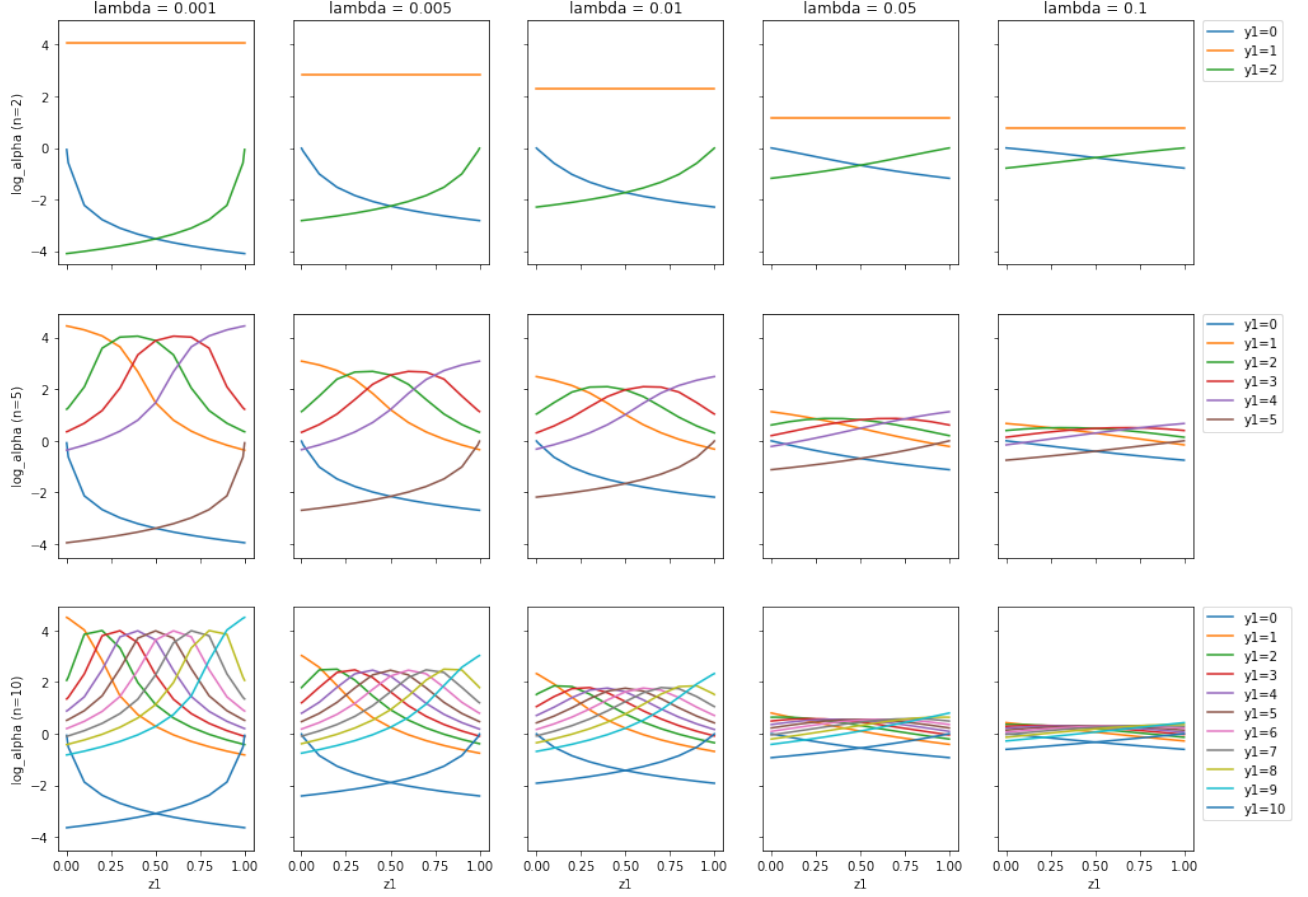

 Optimal values of $\log \alpha_0$ for different values of the hyperparameter λ_α

Figure 3: Optimal values of $\log \alpha_0(x_i)$ are numerically evaluated for binary class problems with the number of labels $n_i \in \{2, 5, 10\}$, label histograms y_i with $0 \leq y_{i1} \leq n_i$, class probability estimations of the first class: $z_1 \in \{.001, .01, .1, .2, \dots, .8, .9, .99, .999\}$, and the hyperparameter λ_α (Appendix D.2). As expected, the range of $\log \alpha_0$ contains zero and gets narrower as λ_α increases.

Hyperparameter analysis for the optimal values of α_0 Intuitively, $\log \alpha_0$ is likely to get close to zero as the regularization coefficient λ_α increases. If we regard $\log \alpha_0(x_i)$ as a free parameter, the optimal value of $\log \alpha_0(x_i)$ only depends on the CPEs $f(x_i)$, the number of labels n_i and the observed labels y_i for each instance. We assume that the number of labels n_i is common for all the instances for simplicity. The optimality condition for α_0 is obtained by taking a derivative of equation (50) with respect to $\log \alpha_0(x_i)$ as follows:

$$\begin{aligned}
 0 &= -\frac{\alpha_0}{n_i} \left[\sum_k f_k (\psi(\alpha_0 f_k + y_{ik}) - \psi(\alpha_0 + n_i)) - \sum_k f_k (\psi(\alpha_0 f_k) - \psi(\alpha_0)) \right] + 2\lambda_\alpha \log \alpha_0 \\
 &= -\frac{\alpha_0}{n_i} \left(\sum_k \sum_{l=1}^{y_{ik}} \frac{f_k}{\alpha_0 f_k + l - 1} - \sum_{l=1}^{n_i} \frac{1}{\alpha_0 + l - 1} \right) + 2\lambda_\alpha \log \alpha_0, \tag{51}
 \end{aligned}$$

where $\psi(\cdot)$ denotes the digamma function, and a recurrence formula $\psi(s+1) = \psi(s) + \frac{1}{s}$ is used for the derivation.

One can verify that divergences of the optimal $\log \alpha_0$ occur in some special cases with $\lambda_\alpha = 0$. For example, if the labels are unanimous, i.e., $y_{i1} = n_i$, $n_i > 1$, and $f_1 < 1$, the r.h.s. of equation (51) turns out to be positive as follows:

$$-\frac{\alpha_0}{n_i} \sum_{l=1}^{n_i} \left(\frac{f_1}{\alpha_0 f_1 + l - 1} - \frac{1}{\alpha_0 + l - 1} \right) > 0,$$

which implies that $\log \alpha_0 \rightarrow -\infty$. In contrast, if $n_i = 2$, $K = 2$, and $y_{i1} = y_{i2} = 1$, the r.h.s of equation (51) is calculated as follows:

$$-\frac{\alpha_0}{n_i} \left(\frac{2}{\alpha_0} - \frac{1}{\alpha_0} - \frac{1}{\alpha_0 + 1} \right) = -\frac{1}{n_i(\alpha_0 + 1)} < 0,$$

which results in $\log \alpha_0 \rightarrow \infty$.

For a finite $\lambda_\alpha > 0$, the optimal values of $\log \alpha_0$ can be numerically evaluated by Newton's method. We show these values in Fig. 3 for several conditions of binary class problems. As expected, the range of the optimal $\log \alpha_0$ contains zero and gets narrower as λ_α increases.

D.3 Proof for Theorem 1

Restatement of Theorem 1. *There exist intervals for parameter $\alpha_0 \geq 0$, which improve task performances as follows.*

1. For DPEs, $L_{\phi^D, G} \leq L_{\phi^D, G}^{(0)}$ holds when $(1 - 2u_Q + s_Z)/2(u_Q - s_Z) \leq \alpha_0$, and $L_{\phi^D, G}$ takes the minimum value when $\alpha_0 = (1 - u_Q)/(u_Q - s_Z)$, if $u_Q > s_Z$ is satisfied.
2. For posterior CPEs, $EL'_G \leq EL_G^{(0)}$ holds when $(1 - u_Q - EL_G)/2EL_G \leq \alpha_0$, and EL'_G takes the minimum value when $\alpha_0 = (1 - u_Q)/EL_G$, if $EL_G > 0$ is satisfied.

Note that we denote $s_Z := \sum_k Z_k^2$, $u_Q := \mathbb{E}[\sum_k Q_k^2 | G]$, $v_Q := \mathbb{V}[Q_k | G]$, and $EL_G := \mathbb{E}[\sum_k (Z_k - Q_k)^2 | G]$. The optimal α_0 of both tasks coincide to be $\alpha_0 = (1 - u_Q)/v_Q$, if CPEs match the true conditional class probabilities given G , i.e., $Z = \mathbb{E}[Q | G]$.

Proof. We will omit the superscript D from ϕ^D and φ^D for brevity. First, we rewrite φ and Z' in equation (19) as follows:

$$\varphi = \gamma \left(1 - \sum_k Z_k^2 \right), \quad Z'_k = \gamma Z_k + (1 - \gamma) Y_k, \quad (52)$$

where $\gamma := \alpha_0/(\alpha_0 + 1)$. Note that $\gamma \in (0, 1)$ since $\alpha_0 \in (0, +\infty)$. We also introduce the following variables:

$$s_Q := \sum_k \mathbb{E}[Q_k | G]^2, \quad \bar{s}_Q := 1 - s_Q, \quad v_Q := \sum_k \mathbb{V}[Q_k | G], \quad (53)$$

$$u_Q := \sum_k \mathbb{E}[Q_k^2 | G] = s_Q + v_Q, \quad \bar{u}_Q := 1 - u_Q, \quad (54)$$

$$s_Z := \sum_k Z_k^2, \quad \bar{s}_Z := 1 - s_Z, \quad (55)$$

where, all the variables reside within $[0, 1]$ since $Z, Q \in \Delta^{K-1}$.

1. The first statement: DPE

The objective function to be minimized is as follows:

$$L_{\phi, G} = \mathbb{E}[(\phi - \varphi)^2 | G] = (\mathbb{E}[\phi | G] - \varphi)^2 + \mathbb{V}[\phi | G] \quad (56)$$

$$= \mathbb{E}[(\bar{u}_Q - \gamma \bar{s}_Z)^2] + \mathbb{V}[\phi | G], \quad (57)$$

where we use the relation $\mathbb{E}[\phi | G] = \bar{u}_Q$ and $\varphi = \gamma \bar{s}_Z$. Note that only the first term is varied with α_0 , and $L_{\phi, G} \rightarrow L_{\phi, G}^{(0)}$ ($\gamma \rightarrow 1$). The condition for satisfying $L_{\phi, G} \leq L_{\phi, G}^{(0)}$ is found by solving

$$0 = L_{\phi, G} - L_{\phi, G}^{(0)} = (\gamma - 1) \bar{s}_Z \{(\gamma + 1) \bar{s}_Z - 2\bar{u}_Q\} = (\gamma - 1) \bar{s}_Z \{\gamma \bar{s}_Z + \bar{s}_Z - 2\bar{u}_Q\}. \quad (58)$$

$\bar{s}_Z = 0$ and $\gamma \rightarrow 1$ are trivial solutions that correspond to a hard label prediction (*i.e.*, $Z \in e^K$) and $\alpha_0 \rightarrow \infty$, respectively. The remaining condition for $L_{\phi, G} \leq L_{\phi, G}^{(0)}$ is

$$\gamma \in [-1 + 2\bar{u}_Q/\bar{s}_Z, 1), \quad (59)$$

which is feasible when $\bar{u}_Q < \bar{s}_Z$, *i.e.*, $u_Q > s_Z$. In this case,

$$\gamma^* = \bar{u}_Q/\bar{s}_Z \quad (60)$$

is the optimal solution for γ . By using a relation $\alpha_0 = \gamma/(1 - \gamma)$ with equations (59) and (60), the first statement of the theorem is obtained as follows:

$$\alpha_0 \geq \frac{-\bar{s}_Z + 2\bar{u}_Q}{2\bar{s}_Z - 2\bar{u}_Q} = \frac{1 - 2u_Q + s_Z}{2(u_Q - s_Z)}, \quad \alpha_0^* = \frac{\bar{u}_Q}{\bar{s}_Z - \bar{u}_Q} = \frac{1 - u_Q}{u_Q - s_Z}. \quad (61)$$

If $Z = \mathbb{E}[Q|G]$ is satisfied, $s_Z = s_Q$ holds, and the above conditions become as follows:

$$\alpha_0 \geq \frac{1 - u_Q - v_Q}{2v_Q}, \quad \alpha_0^* = \frac{1 - u_Q}{v_Q}. \quad (62)$$

2. The second statement: posterior CPE

The objective for the second problem is as follows:

$$\begin{aligned} \text{EL}'_G &= \mathbb{E}\left[\sum_k (Z'_k - Q_k)^2 | G\right] \\ &= \mathbb{E}\left[\sum_k (\gamma Z_k + (1 - \gamma)Y_k - Q_k)^2 | G\right] \\ &= \mathbb{E}\left[\sum_k ((Z_k - Q_k) + (1 - \gamma)(Y_k - Z_k))^2 | G\right] \\ &= \sum_k \mathbb{E}[(Z_k - Q_k)^2 | G] + 2(1 - \gamma) \mathbb{E}[(Z_k - Q_k)(Y_k - Z_k) | G] + (1 - \gamma)^2 \mathbb{E}[(Y_k - Z_k)^2 | G], \end{aligned} \quad (63)$$

where the first term equals to EL_G , and the second and third term are further transformed as follows:

$$\begin{aligned} \sum_k \mathbb{E}[(Z_k - Q_k)(Y_k - Z_k) | G] &= \sum_k \mathbb{E}[\mathbb{E}[(Z_k - Q_k)(Y_k - Z_k) | Q] | G] \\ &= - \sum_k \mathbb{E}[\mathbb{E}[(Z_k - Q_k)^2 | Q] | G] = -\text{EL}_G, \\ \sum_k \mathbb{E}[(Y_k - Z_k)^2 | G] &= \sum_k \mathbb{E}[\mathbb{E}[(Y_k - Z_k)^2 | Q] | G] \\ &= \sum_k \mathbb{E}[\mathbb{E}[(Y_k - 2Y_k Z_k + Z_k^2) | Q] | G] \\ &= \sum_k \mathbb{E}[(Q_k - 2Q_k Z_k + Z_k^2) | G] \\ &= \sum_k \mathbb{E}[(Q_k(1 - Q_k) + (Q_k - Z_k)^2) | G] = \bar{u}_Q + \text{EL}_G. \end{aligned} \quad (64)$$

Hence equation (63) can be written as

$$\text{EL}'_G = \text{EL}_G - 2(1 - \gamma) \text{EL}_G + (1 - \gamma)^2 (\text{EL}_G + \bar{u}_Q). \quad (66)$$

The condition for satisfying $\text{EL}'_G \leq \text{EL}_G$ is obtained by solving

$$0 = \text{EL}'_G - \text{EL}_G = (1 - \gamma) \{(1 - \gamma)(\text{EL}_G + \bar{u}_Q) - 2\text{EL}_G\}. \quad (67)$$

If $\text{EL}_G = 0$, which means $Z_k = Q_k$ given G , $\gamma \rightarrow 1$ is optimal as expected. For the other case, *i.e.*, $\text{EL}_G > 0$, γ that satisfying $\text{EL}'_G \leq \text{EL}_G$ and the optimal γ are

$$\gamma \in \left[\frac{\bar{u}_Q - \text{EL}_G}{\bar{u}_Q + \text{EL}_G}, 1 \right), \quad \gamma^* = \frac{\bar{u}_Q}{\bar{u}_Q + \text{EL}_G}, \quad (68)$$

respectively. By using $\alpha_0 = \gamma/(1 - \gamma)$, the corresponding α_0 and α_0^* are

$$\alpha_0 \geq \frac{\bar{u}_Q - \text{EL}_G}{2 \text{EL}_G} = \frac{1 - u_Q - \text{EL}_G}{2 \text{EL}_G}, \quad \alpha_0^* = \frac{\bar{u}_Q}{\text{EL}_G} = \frac{1 - u_Q}{\text{EL}_G}, \quad (69)$$

respectively, which are the second statement of the theorem. If $Z = \mathbb{E}[Q|G]$ is satisfied, $\text{EL}_G = v_Q$ holds, and the above conditions become as follows:

$$\alpha_0 \geq \frac{1 - u_Q - v_Q}{2v_Q}, \quad \alpha_0^* = \frac{1 - u_Q}{v_Q}. \quad (70)$$

Notably, these are the same conditions as the terms in equation (62), respectively. \square

D.4 Summary of DPE computations

We use α -calibration, ensemble-based methods (MCDO and TTA), and a combination of them for predicting DPEs as follows.

α -calibration

$$\hat{\varphi}^D = 1 - \sum_k \int \zeta_k^2 \text{Dir}(\zeta | \alpha_0 f) d\zeta = \frac{\alpha_0}{\alpha_0 + 1} \left(1 - \sum_k f_k^2 \right). \quad (71)$$

Ensemble-based methods

$$\hat{\varphi}^D = \frac{1}{S} \sum_{s=1}^S \left(1 - \sum_k \left(f_k^{(s)} \right)^2 \right), \quad (72)$$

where, $f^{(s)} : \mathcal{X} \rightarrow \Delta^{(k-1)}$ is the s -th prediction of the ensemble, and S is the size of the ensemble.

Ensemble-based methods with α -calibration Although an output α already represents a CPE distribution without ensemble-based methods: MCDO and TTA, it can be formally combined with these methods. In such cases, we calculate the predictive probability $\hat{\varphi}$ as follows:

$$\hat{\varphi}^D = \frac{1}{S} \sum_{s=1}^S \left[\frac{\alpha_0^{(s)}}{\alpha_0^{(s)} + 1} \left(1 - \sum_k \left(f_k^{(s)} \right)^2 \right) \right], \quad (73)$$

where $\alpha_0^{(s)}$, $f^{(s)}$ denote the s -th ensembles of α_0 and f , respectively.

D.5 Summary of posterior CPE computations

We consider a task for updating CPE of instance $x \in \mathcal{X}$ after an expert annotation $y \in e^K$. For this task, the posterior CPE distribution $P_{\text{model}}(\zeta|x, y)$ is computed from an original (prior) CPE distribution model $P_{\text{model}}(\zeta|x)$ as follows:

$$P_{\text{model}}(\zeta|x, y) = \frac{P_{\text{model}}(y, \zeta|x)}{P_{\text{model}}(y|x)}, \quad (74)$$

where

$$P_{\text{model}}(y, \zeta|x) = P_{\text{model}}(\zeta|x) \prod_{k=1}^K \zeta_k^{y_k}. \quad (75)$$

For the case with multiple test instances, we assume that a predictive model is factorized as follows:

$$P_{\text{model},N}(\zeta_{1:N}|x_{1:N}) = \prod_{i=1}^N P_{\text{model}}(\zeta_i|x_i). \quad (76)$$

In this case, the posterior of CPEs is also factorized as follows:

$$P_{\text{model},N}(\zeta_{1:N}|x_{1:N}, y_{1:N}) = \frac{P_{\text{model},N}(y_{1:N}, \zeta_{1:N}|x_{1:N})}{P_{\text{model},N}(y_{1:N}|x_{1:N})} = \prod_{i=1}^N \frac{P_{\text{model}}(y_i, \zeta_i|x_i)}{P_{\text{model}}(y_i|x_i)} = \prod_{i=1}^N P_{\text{model}}(\zeta_i|x_i, y_i). \quad (77)$$

α -calibration Prior and posterior CPE distributions are computed as follows:

$$P_{\alpha}(\zeta|x) = \text{Dir}(\zeta|\alpha_0(x)f(x)), \quad (78)$$

$$P_{\alpha}(\zeta|x, y) = \text{Dir}(\zeta|\alpha_0(x)f(x) + y). \quad (79)$$

Ensemble-based methods Prior and posterior CPE distributions are computed as follows:

$$P_{\text{ens.}}(\zeta|x) = \frac{1}{S} \sum_{s=1}^S \delta(\zeta - f^{(s)}(x)), \quad (80)$$

$$P_{\text{ens.}}(\zeta|x, y) = \frac{1}{W'} \sum_{s=1}^S w'_s \delta(\zeta - f^{(s)}(x)), \quad (81)$$

where S is the size of the ensemble, $f^{(s)}$ denotes the s -th CPEs of the ensemble, $w'_s := \sum_s \prod_k f^{(s)}(x)_k^{y_k}$, and $W' := \sum_{s=1}^S w'_s$.

We omit the cases of predictive models combining the ensemble-based methods and α -calibration, where the posterior computation requires further approximation.

D.6 Discussion on conditional i.i.d. assumption of label generations for α -calibration

At the beginning of section 3, we assume a conditional i.i.d distribution for labels Y given input data X , which is also a basis for α -calibration. We expect that the assumption roughly holds in typical scenarios, where experts are randomly assigned to each example. However, α -calibration may not be suitable for counter-examples that break the assumption. For instance, if two fixed experts with different policy annotate all examples, these two labels would be highly correlated. In such a case, the disagreement probability between them may be up to one and exceeds the maximum possible value φ^{D} allowed in equation (19), where φ^{D} always decreases from the original value, which corresponds to $\alpha_0 \rightarrow \infty$, by α -calibration.

E Experimental details

We used the Keras Framework with Tensorflow backend (Chollet et al., 2015) for implementation.

E.1 Preprocessing

Mix-MNIST and CIFAR-10 We generated two synthetic image dataset: Mix-MNIST and Mix-CIFAR-10 from MNIST (LeCun et al., 2010) and CIFAR-10 (Krizhevsky et al., 2009), respectively. We randomly selected half of the images to create mixed-up images from pairs and the other half were retained as original. For each of the paired images, a random ratio that followed a uniform distribution $U(0, 1)$ was used for the mix-up and a class probability of multiple labels, which were two or five in validation set. For Mix-MNIST (Mix-CIFAR-10), the numbers of generated instances were 37, 500 (30, 000), 7, 500 (7, 500), and 7, 500 (7, 500) for training, validation, and test set, respectively.

MDS Data We used 80,610 blood cell images with a size of 360×363 , which was a part of the dataset obtained in a study of myelodysplastic syndrome (MDS) (Sasada et al., 2018), where most of the images showed a white blood cell in the center of the image. For each image, a mean of 5.67 medical technologists annotated the cellular category from 22 subtypes, in which six were anomalous types. We partitioned the dataset into training, validation, and test set with 55,356, 14,144, and 11,110 images, respectively, where each of the partition consisted of images from distinct patient groups. Considering the high labeling cost with experts in the medical domain, we focused on scenarios that training instances were singly labeled, and multiple labels were only available for validation and test set. The mean number of labels per instance for validation and test set were 5.79 and 7.58, respectively.

E.2 Deep neural network architecture

Mix-MNIST For Mix-MNIST dataset, we used a neural network architecture with three convolutional and two full connection layers. Specifically, the network had the following stack:

- Conv. layer with 32 channels, 5×5 kernel, and ReLU activation
- Max pooling with 2×2 kernel and same padding
- Conv. layer with 64 channels, 7×7 kernel, and ReLU activation
- Max pooling with 4×4 kernel and same padding
- Conv. layer with 128 channels, 11×11 kernel, and ReLU activation
- Global average pooling with 128 dim. output
- Dropout with 50% rate
- Full connection layer with $K = 3$ dim. output and softmax activation

Mix-CIFAR-10 and MDS We adopted a modified VGG16 architecture (Simonyan and Zisserman, 2014) as a base model, in which the full connection layers were removed, and the last layer was a max-pooling with 512 output dimensions. On top of the base model, we appended the following layers:

- Dropout with 50% rate and 512 dim. output
- Full connection layer with 128 dim. output and ReLU activation
- Dropout with 50% rate and 128 dim. output
- Full connection layer with 22 dim. output and softmax activation

E.3 Training

We used the following loss function for training:

$$\mathcal{L}(y, z) = -\frac{1}{\sum_{i=1}^N n_i} \sum_{i=1}^N \sum_{k=1}^K y_{ik} \log z_{ik}, \tag{82}$$

which was equivalent to the negative log-likelihood for instance-wise multinomial observational model except for constant. We used Adam optimizer (Kingma and Ba, 2014) with a base learning rate of 0.001. Below, we summarize conditions specific to each dataset.

Mix-MNIST We trained for a maximum of 100 epochs with a minibatch size of 128, applying early stopping with ten epochs patience for the validation loss improvement. We used no data augmentation for Mix-MNIST.

Mix-CIFAR-10 We trained for a maximum of 250 epochs with a minibatch size of 128, applying a variant of warm-up and multi-step decay scheduling (He et al., 2016) as follows:

- A warm-up with five epochs
- A multi-step decay that multiplies the learning rate by 0.1 at the end of 100 and 150 epochs

We selected the best weights in terms of validation loss. While training, we applied data augmentation with random combinations of the following transformations:

- Rotation within -180 to 180 degrees
- Width and height shift within ± 10 pixels
- Horizontal flip

MDS We trained for a maximum of 200 epochs with a minibatch size of 128, applying a warm-up and multi-step decay scheduling as follows:

- A warm-up with five epochs
- A multi-step decay that multiplies the learning rate by 0.1 at the end of 50, 100, and 150 epochs

We recorded training weights for every five epochs, and selected the best weights in terms of validation loss. While training, we applied data augmentation with random combinations of the following transformations:

- Rotation within -20 to 20 degrees
- Width and height shift within ± 5 pixels
- Horizontal flip

For each image, the center 224×224 portion is cropped from the image after the data augmentation.

E.4 Post-hoc calibrations and predictions

We applied temperature scaling for CPE calibration and α -calibration for obtaining CPE distributions. For both calibration methods, we used validation set, which was split into 80% calibration set for training and 20% calibration-validation (cv) set for the validation of calibration. We trained for a maximum of 50 epochs using Adam optimizer with a learning rate of 0.001, applying early stopping with ten epochs patience for the cv loss improvement. The loss functions of equation (82) and (50) were used for CPE- and α -calibration, respectively. For the feature layer that used for α -calibration, we chose the penultimate layer that corresponded to the last dropout layer in this experiment. The training scheme is the same as that of the CPE calibration, except for a loss function that we described in D.2. We also used ensemble-based methods: Monte-Carlo dropout (MCDO) (Gal and Ghahramani, 2016) and Test-time augmentation (TTA) (Ayhan and Berens, 2018) for CPE distribution predictions, which were both applicable to DNNs at prediction-time, where 20 MC-samples were used for ensemble. A data augmentation applied in TTA was the same as that used in training, and we only applied TTA for Mix-CIFAR-10 and MDS data.

F Additional experiments

F.1 Evaluations of class probability estimates

We present evaluation results of class probability estimates (CPEs) for Mix-MNIST and Mix-CIFAR-10 in Table 4 and 5, respectively. Overall, CPE measures were comparable between the same datasets with different validation labels (two and five). By comparing \widehat{L}_{sq} and \widehat{EL} , the relative ratio of \widehat{EL} against irreducible loss could be evaluated which was much higher in Mix-CIFAR-10 than in Mix-MNIST. Among Raw predictions, temperature scaling kept accuracy and showed a consistent improvement in \widehat{EL} and \widehat{CE} as expected. While TTA showed a superior performance over MCDO and Raw predictions in accuracy, \widehat{L}_{sq} and \widehat{EL} , the effect of calibration methods for CPEs with ensemble-based predictions was not consistent, which might be because calibration was not ensemble-aware.

F.2 Discussion on the effect of temperature scaling for disagreement probability estimates

In Table 1, it is observed that disagreement probability estimates (DPEs) are consistently degraded by temperature scaling (Raw+ts) from the original scores (Raw), despite the positive effects for calibration of class probability estimates (CPEs) with ts. Though we observe that the degradation can be overcome with α -calibration (see Raw+ts+ α or Raw+ α in Table 1), the mechanism that causes the phenomena is worth analyzing. Since there exists well-known overconfidence in the maximum class probabilities from DNN classifiers (Guo et al., 2017), the recalibration of CPEs by ts tends to reduce the maximum class probabilities. On the other hand, the amount of change in a DPE for each instance can be written as follows:

$$\Delta^D := \varphi^D - \varphi^D = \sum_{k=1}^K (f_k + f'_k)(f_k - f'_k), \quad (83)$$

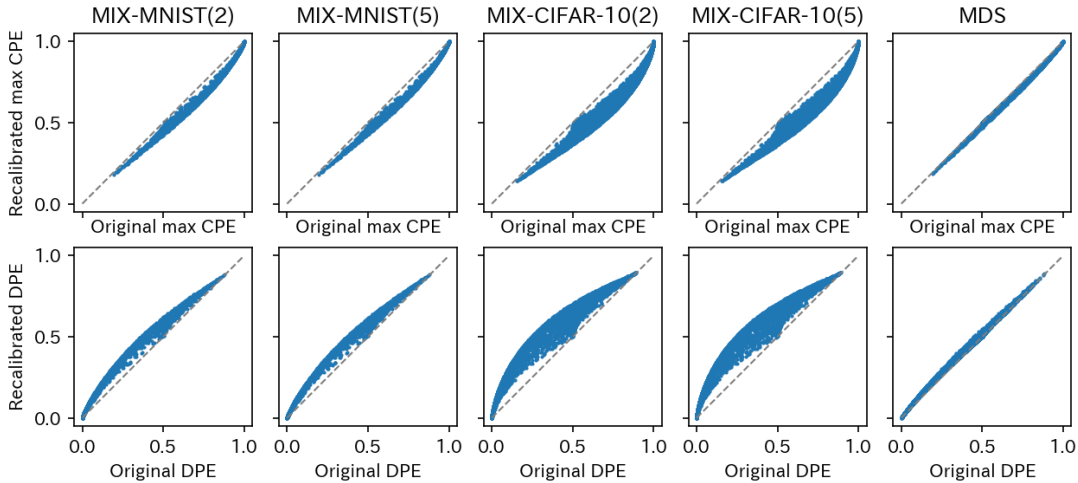
where f and φ^D denote the original CPEs and DPE, respectively, and f' and φ'^D denote those after ts, respectively. It is likely that Δ^D takes a positive value as the dominant term of Δ^D in equation (83) is k with the maximum $f_k + f'_k$ value, where $f_k > f'_k$ is satisfied for overconfident predictions. In fact, the averages of Δ^D between Raw+ts and Raw for each of the five settings in Table 1 are all positive, which are 0.027, 0.025, 0.101, 0.103, and 0.019, respectively. Instance-wise changes in the maximum CPEs and DPEs with ts are shown in Fig. 4. Simultaneously, DPEs without α -calibration systematically overestimate the empirical disagreement probabilities, as shown in Fig. 1. Therefore, the positive Δ^D means that φ'^D is even far from a target probability $\mathbb{E}[\phi^D|X]$ than φ^D is, despite the improvement in CPEs with ts.

Table 4: Evaluations of CPEs for Mix-MNIST

Method	Mix-MNIST(2)				Mix-MNIST(5)			
	Acc \uparrow	\widehat{L}_{sq} \downarrow	\widehat{EL} \downarrow	\widehat{CE} \downarrow	Acc \uparrow	\widehat{L}_{sq} \downarrow	\widehat{EL} \downarrow	\widehat{CE} \downarrow
Raw	.9629	.1386	.0388	.0518	.9629	.1386	.0388	.0518
Raw+ α	.9629	.1386	.0388	.0518	.9629	.1386	.0388	.0518
Raw+ts	.9629	.1376	.0379	.0473	.9629	.1376	.0379	.0475
Raw+ts+ α	.9629	.1376	.0379	.0473	.9629	.1376	.0379	.0475
MCDO	.9635	.1392	.0395	.0425	.9635	.1392	.0395	.0425
MCDO+ α	.9621	.1391	.0394	.0442	.9644	.1387	.0389	.0463
MCDO+ts	.9628	.1408	.0410	.0632	.9627	.1402	.0404	.0638
MCDO+ts+ α	.9624	.1412	.0415	.0653	.9629	.1407	.0409	.0631

Table 5: Evaluations of CPEs for Mix-CIFAR-10

Method	Mix-CIFAR-10(2)				Mix-CIFAR-10(5)			
	Acc \uparrow	\widehat{L}_{sq} \downarrow	\widehat{EL} \downarrow	\widehat{CE} \downarrow	Acc \uparrow	\widehat{L}_{sq} \downarrow	\widehat{EL} \downarrow	\widehat{CE} \downarrow
Raw	.7965	.3518	.2504	.1093	.7965	.3518	.2504	.1093
Raw+ α	.7965	.3518	.2504	.1093	.7965	.3518	.2504	.1093
Raw+ts	.7965	.3437	.2423	.0687	.7965	.3438	.2423	.0685
Raw+ts+ α	.7965	.3437	.2423	.0688	.7965	.3438	.2423	.0685
MCDO	.7983	.3488	.2474	.0955	.7983	.3488	.2474	.0955
MCDO+ α	.7968	.3488	.2474	.0962	.7965	.3493	.2479	.0973
MCDO+ts	.7972	.3442	.2428	.0684	.7977	.3446	.2431	.0675
MCDO+ts+ α	.7965	.3445	.2430	.0650	.7975	.3444	.2430	.0723
TTA	.8221	.3230	.2216	.0877	.8221	.3230	.2216	.0877
TTA+ α	.8241	.3221	.2206	.0884	.8277	.3223	.2209	.0894
TTA+ts	.8257	.3467	.2452	.1688	.8279	.3466	.2451	.1707
TTA+ts+ α	.8277	.3446	.2432	.1697	.8245	.3460	.2446	.1726



Changes in the maximum CPEs and DPEs with temperature scaling

Figure 4: Changes in the maximum class probability estimates (CPEs) and disagreement probability estimates (DPEs) with temperature scaling (t_s) are presented for each instance. In contrast to the maximum CPEs, which are generally decreased with t_s to compensate overconfidence, DPEs are increased with t_s as discussed in Appendix F.2.

F.3 Additional experiments for MDS data

In addition to MDS data with single training labels per instance (MDS-1) used in the main experiment, we trained and evaluated with full MDS data (MDS-full), where all the multiple training labels per example were employed. Also, we included additional CPE calibration methods: vector and matrix scaling (vs and ms, respectively), which were introduced in Section D.1, for these experiments. We adopted an L2 regularization for vs and an ODIR for ms, in which the following hyper-parameter candidates were examined:

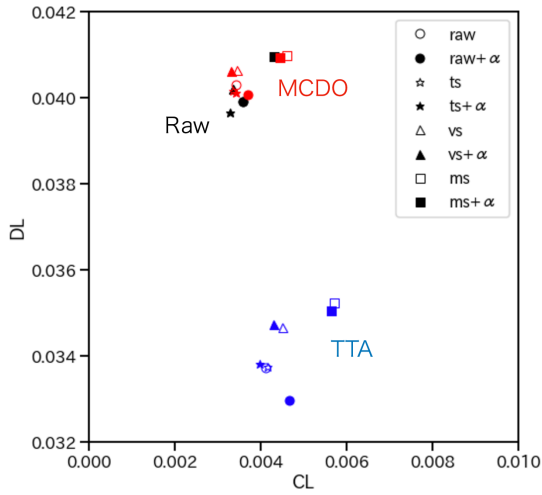
- vs: $\lambda_b \in \{0.1, 1.0, 10\}$
- ms: $(\lambda_b, \lambda_w) \in \{0.1, 1.0, 10\} \times \{0.1, 1.0, 10\}$

where λ_b and λ_w were defined in equation (48) and (49), respectively. The hyper-parameters were selected with respect to the best cv loss, which were $\lambda_b = 0.1$ for vs and $\lambda_b = 1.0, \lambda_w = 10$ for ms in the single-training MDS data, and $\lambda_b = 0.1$ for vs and $\lambda_b = 0.1, \lambda_w = 10$ for ms in the full MDS data.

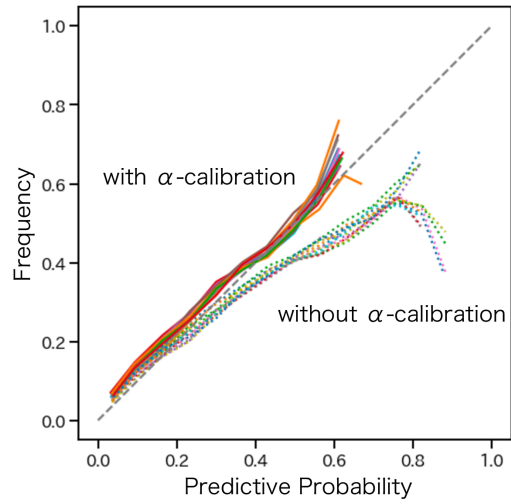
Results We summarize the order-1 and -2 performance metrics for predictions with MDS-1 and MDS-full datasets in Table 6. For both datasets, temperature scaling consistently improved (decreased) \widehat{EL} and \widehat{CL} for each of Raw, MCDO, and TTA predictions. While vector scaling was slightly better at obtaining the highest accuracy than the other methods, the effect of vs and ms for the metrics of probability predictions were limited. As same as the results of synthetic experiments, TTA showed a superior performance over MCDO and Raw predictions in accuracy, \widehat{L}_{sq} and \widehat{EL} . Since \widehat{EL} can be decomposed into \widehat{CL} and the remaining term: \widehat{DL} (Section B.4), the difference of predictors in CPE performance is clearly presented with 2d plots (Fig.5 and 6), which we call calibration-dispersion maps. For order-2 metrics, both \widehat{L}_{ϕ^D} and \widehat{CE}_{ϕ^D} for DPEs were substantially improved by α -calibration, especially in \widehat{CE}_{ϕ^D} , which was not attained with solely applying ensemble-based methods even with MDS-full. This improvement of DPE calibration was also visually confirmed with reliability diagrams in Fig. 5 and 6. Though overall characteristics were similar between MDS-1 and MDS-full, a substantial improvement in \widehat{L}_{sq} , \widehat{EL} , and \widehat{L}_{ϕ^D} was observed in MDS-full, which seemed the results of enhanced probability predictions with additional training labels.

Table 6: Performance evaluations for MDS data

Method	MDS-1												MDS-full											
	Order-1 metrics				Order-2 metrics				Order-1 metrics				Order-2 metrics											
	Acc \uparrow	$\hat{L}_{sq} \downarrow$	$\widehat{EL} \downarrow$	$\widehat{CE} \downarrow$	$\hat{L}_{\phi,D} \downarrow$	$\widehat{CE}_{\phi,D} \downarrow$	Acc \uparrow	$\hat{L}_{sq} \downarrow$	$\widehat{EL} \downarrow$	$\widehat{CE} \downarrow$	$\hat{L}_{\phi,D} \downarrow$	$\widehat{CE}_{\phi,D} \downarrow$	Acc \uparrow	$\hat{L}_{sq} \downarrow$	$\widehat{EL} \downarrow$	$\widehat{CE} \downarrow$	$\hat{L}_{\phi,D} \downarrow$	$\widehat{CE}_{\phi,D} \downarrow$						
Raw	.9006	.2515	.0435	.0600	.1477	.0628	.8990	.2460	.0380	.0590	.1448	.0539	.8990	.2460	.0380	.0590	.1448	.0539						
Raw+ α	.9006	.2515	.0435	.0600	.1454	.0406	.8990	.2460	.0380	.0590	.1430	.0320	.8990	.2460	.0380	.0590	.1430	.0320						
Raw+ts	.9006	.2509	.0430	.0575	.1482	.0663	.8990	.2459	.0379	.0587	.1449	.0545	.8990	.2459	.0379	.0587	.1449	.0545						
Raw+ts+ α	.9006	.2509	.0430	.0575	.1445	.0261	.8990	.2459	.0379	.0587	.1427	.0269	.8990	.2459	.0379	.0587	.1427	.0269						
Raw+vs	.9010	.2515	.0435	.0579	.1489	.0696	.8996	.2461	.0381	.0602	.1452	.0563	.8996	.2461	.0381	.0602	.1452	.0563						
Raw+vs+ α	.9010	.2515	.0435	.0579	.1449	.0318	.8996	.2461	.0381	.0602	.1431	.0310	.8996	.2461	.0381	.0602	.1431	.0310						
Raw+ms	.8992	.2532	.0453	.0656	.1484	.0663	.8978	.2480	.0400	.0710	.1451	.0563	.8978	.2480	.0400	.0710	.1451	.0563						
Raw+ms+ α	.8992	.2532	.0453	.0656	.1453	.0355	.8978	.2480	.0400	.0710	.1428	.0274	.8978	.2480	.0400	.0710	.1428	.0274						
MCDO	.8983	.2517	.0437	.0586	.1470	.0562	.8989	.2460	.0380	.0561	.1446	.0505	.8989	.2460	.0380	.0561	.1446	.0505						
MCDO+ α	.8996	.2518	.0438	.0610	.1450	.0346	.9003	.2458	.0378	.0568	.1426	.0237	.9003	.2458	.0378	.0568	.1426	.0237						
MCDO+ts	.8986	.2515	.0435	.0579	.1479	.0635	.8995	.2458	.0378	.0579	.1447	.0521	.8995	.2458	.0378	.0579	.1447	.0521						
MCDO+ts+ α	.8991	.2515	.0435	.0586	.1442	.0186	.8997	.2460	.0380	.0581	.1423	.0180	.8997	.2460	.0380	.0581	.1423	.0180						
MCDO+vs	.8997	.2521	.0441	.0589	.1487	.0664	.9004	.2461	.0381	.0593	.1448	.0531	.9004	.2461	.0381	.0593	.1448	.0531						
MCDO+vs+ α	.9009	.2519	.0439	.0575	.1446	.0244	.9002	.2460	.0380	.0579	.1426	.0228	.9002	.2460	.0380	.0579	.1426	.0228						
MCDO+ms	.8970	.2536	.0456	.0678	.1479	.0612	.8997	.2477	.0397	.0704	.1448	.0529	.8997	.2477	.0397	.0704	.1448	.0529						
MCDO+ms+ α	.8986	.2534	.0454	.0667	.1449	.0279	.8986	.2478	.0399	.0695	.1424	.0188	.8986	.2478	.0399	.0695	.1424	.0188						
TTA	.9013	.2458	.0378	.0642	.1441	.0488	.9069	.2402	.0322	.0645	.1425	.0444	.9069	.2402	.0322	.0645	.1425	.0444						
TTA+ α	.9025	.2456	.0376	.0684	.1428	.0334	.9077	.2402	.0322	.0650	.1413	.0277	.9077	.2402	.0322	.0650	.1413	.0277						
TTA+ts	.9012	.2459	.0379	.0646	.1448	.0553	.9074	.2401	.0321	.0636	.1425	.0456	.9074	.2401	.0321	.0636	.1425	.0456						
TTA+ts+ α	.9011	.2458	.0378	.0632	.1422	.0197	.9055	.2403	.0323	.0633	.1410	.0204	.9055	.2403	.0323	.0633	.1410	.0204						
TTA+vs	.9031	.2471	.0392	.0671	.1458	.0598	.9078	.2409	.0329	.0666	.1431	.0483	.9078	.2409	.0329	.0666	.1431	.0483						
TTA+vs+ α	.9025	.2470	.0391	.0657	.1428	.0247	.9068	.2409	.0329	.0664	.1416	.0252	.9068	.2409	.0329	.0664	.1416	.0252						
TTA+ms	.9001	.2489	.0410	.0756	.1456	.0561	.9034	.2429	.0349	.0778	.1431	.0481	.9034	.2429	.0349	.0778	.1431	.0481						
TTA+ms+ α	.8991	.2487	.0407	.0750	.1431	.0268	.9030	.2432	.0352	.0766	.1414	.0213	.9030	.2432	.0352	.0766	.1414	.0213						

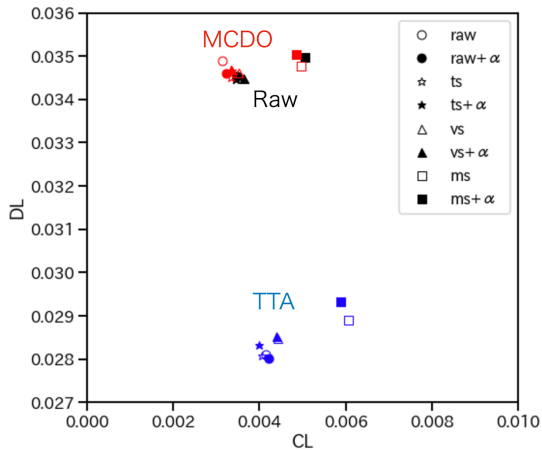


(a) Calibration-dispersion map

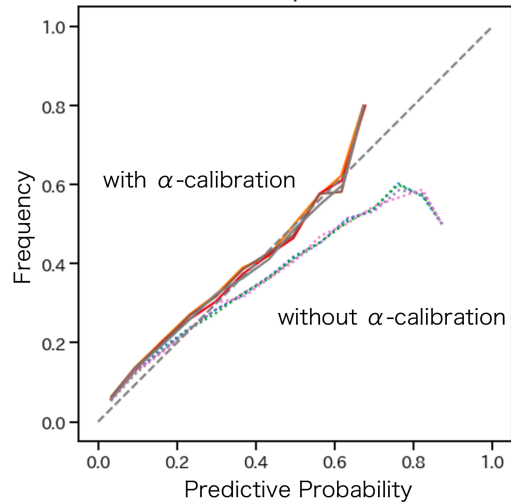


(b) Reliability diagram for disagreement probability

Figure 5: (a) Calibration-dispersion map for the experiments with MDS-1 data. (b) Reliability diagram of disagreement probability estimates (DPEs) for MDS-1 data, where all the predictive methods in Table 6 were compared. The dashed diagonal line corresponds to a calibrated prediction. Calibration of DPEs was significantly enhanced with α -calibration (solid lines) from the original ones (dotted lines).



(a) Calibration-dispersion map



(b) Reliability diagram for disagreement probability

Figure 6: (a) Calibration-dispersion map for the experiments with MDS-full data. (b) Reliability diagram of disagreement probability estimates (DPEs) for MDS-full data, where all the predictive methods in Table 6 were compared. The dashed diagonal line corresponds to a calibrated prediction.